

**UNIVERSITY OF GAZİANTEP
GRADUATE SCHOOL OF
NATURAL & APPLIED SCIENCES**

**A NEW APPROACH FOR DETERMINING STATISTICAL
DISTRIBUTION OF IMPULSE BREAKDOWN VOLTAGE
UNDER EXTERNAL ELECTRICAL EFFECTS**

**M. Sc. THESIS
IN
ELECTRICAL-ELECTRONICS ENGINEERING**

**BY
MEHMET DEMİR
SEPTEMBER 2012**

**A New Approach For Determining Statistical Distribution Of
Impulse Breakdown Voltage Under External Electrical Effects**

M. Sc. Thesis
in
Electrical-Electronics Engineering
University of Gaziantep

Supervisor
Prof. Dr. Celal KORAŞLI

by
Mehmet DEMİR
September 2012

©2012[MehmetDEMİR]

REPUBLIC OF TURKEY
UNIVERSITY OF GAZİANTEP
GRADUATE SCHOOL OF NATURAL & APPLIED SCIENCES
ELECTRICAL-ELECTRONICS ENGINEERING

Name of the thesis: A new approach for determining statistical distribution of impulse breakdown voltage under external electrical effects


Name of the student: Mehmet DEMİR

Exam date: 04.09.2012

Approval of the Graduate School of Natural and Applied Sciences


Prof. Dr. Ramazan KOÇ
Director

I certify that this thesis satisfies all the requirements as a thesis for the degree of Master of Science.


Prof. Dr. Celal KORAŞLI
Head of Department

This is to certify that we have read this thesis and that in our consensus/majority opinion it is fully adequate, in scope and quality, as a thesis for the degree of Master of Science.

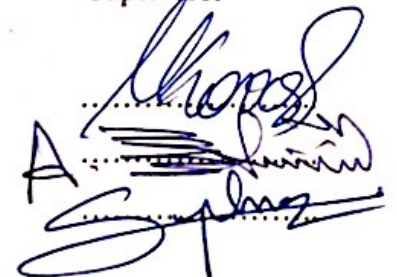

Prof. Dr. Celal KORAŞLI
Supervisor

Examining Committee Members (Title and Name-surname)

Prof. Dr. Celal KORAŞLI

Prof. Dr. A.Necmettin YAZICI

Assoc. Prof. Dr. A.Serdar YILMAZ



I hereby declare that all information in this document has been obtained and presented in accordance with academic rules and ethical conduct. I also declare that, as required by these rules and conduct, I have fully cited and referenced all material and results that are not original to this work.

Mehmet DEMİR

ABSTRACT

A NEW APPROACH FOR DETERMINING STATISTICAL DISTRIBUTION OF IMPULSE BREAKDOWN VOLTAGE UNDER EXTERNAL ELECTRICAL EFFECTS

DEMİR, Mehmet

M.Sc. in Electrical-Electronics Eng.

Supervisor: Prof. Dr. Celal KORAŞLI

September 2012, 70 pages

This study presents a comprehensive approach to statistical characterization of impulse breakdown voltage under the influence of DC sweep voltage. Several goodness-of-fit procedures are applied to the up-and-down test results which are obtained experimentally with and without a sweep field in air-insulated rod-plane gap system in order to decide upon the the type of impulse breakdown voltage distribution. Three distributions; Normal, logistic and Gumbel distributions are compared by means of Kolmogorov-Smirnov (K-S) goodness-of-fit test. Logistic distribution fits better than other two distributions for all positive impulse breakdown voltage data in the existence of sweep voltages. Logistic distribution is also compared with three-parameter Weibull (3PW) distribution by using likelihood ratio (LR) test. Consequently, logistic distribution can be accepted as an alternative to normal and 3PW distributions.

The statistical time-lag distribution of positive impulse breakdown voltage under various DC sweep voltages was also investigated using the 'Laue' plot technique. Time-lag distributions of the impulse breakdown voltage data generally found to exhibit no definitive statistical variation but it seems an exponential type distribution can be applied to characterize the data.

Keywords: Sweep voltage, swing-motion impulse generator, Kolmogorov-Smirnov test, likelihood ratio test, 50% impulse breakdown voltage, Monte-Carlo optimization, logistic distribution.

ÖZET
HARİCİ ELEKTRİKSEL ETKİ ALTINDA DARBE DELİNME
GERİLİMİNİN İSTATİKSEL DAĞILIMINI BELİRLEMEK İÇİN YENİ BİR
YAKLAŞIM

DEMİR, Mehmet

Yüksek Lisans Tezi, Elektrik-Elektronik Müh. Bölümü

Tez Yöneticisi: Prof. Dr. Celal KORAŞLI

Eylül 2012, 70 sayfa

Bu çalışma DC süpürme gerilimi etkisi altındaki darbe delinme geriliminin istatistiksel karakterizasyonu hakkında geniş kapsamlı yaklaşım sunmaktadır. Darbe delinme gerilim dağılımının tipine karar vermek için, birkaç uyum iyiliği testleri hava izolasyonlu çubuk-düzlem elektrot sisteminde DC süpürme gerilimli ve DC süpürme gerilimi olmadan deneysel olarak elde edilen up-and-down test sonuçlarına uygulanmıştır. Üç istatistiksel dağılım; Normal, lojistik ve Gumbel dağılımları Kolmogorov-Smirnov (K-S) uyum iyiliği testi ile karşılaştırılmıştır. DC süpürme gerilimi varlığında bütün pozitif darbe delinme gerilim verilerine lojistik dağılım diğer iki dağılımdan daha iyi uyumuştur. Ayrıca lojistik dağılım olasılık oran testi (OOT) kullanılarak üç parametrelili Weibull (ÜPW) ile karşılaştırılmıştır. Bu testlerin sonucunda lojistik dağılımın normal ve ÜPW dağılımlarına alternatif olabileceği kabul edilmiştir.

Çeşitli DC süpürme geriliminin etkisi altında elde edilen pozitif darbe delinme gerilim verilerinin istatistiksel zaman gecikme dağılımı 'Laue' grafik tekniği ile incelenmiştir. Zaman gecikme dağılımlarının kesin bir istatistiksel değişim göstermediği bulunmuştur ama zaman gecikme dağılımlarını karakterize etmek için eksponansiyel dağılım uygulanabileceği görülmektedir.

Anahtar Kelimeler: Süpürme gerilimi, dönel hareket ateşlemeli darbe jeneratörü, Kolmogorov-Smirnov test, olasılık oran testi, 50% darbe delinme gerilimi, Monte-Carlo optimizasyon, lojistik dağılım.

To My Mother and Father

ACKNOWLEDGEMENTS

First and foremost, I would like to thank the Most Merciful Allah for giving me the strength to complete this study.

I would like to express my deepest gratitude to my supervisor Prof. Dr. Celal KORAŞLI for his excellent guidance, caring, patience and insight throughout this study.

It gives me great pleasure in acknowledging the support and help of Assoc. Prof. Dr. Ali İhsan GENÇ, Assist. Prof. Dr. Andrew BEDDALL and Assist. Prof. Dr. Ahmet BİNGÜL.

I would also like to thank to my friends Seydi KAÇMAZ, Ali Osman ARSLAN, Mehmet ARICI, Erhan ERSOY and Mahmut AYKAÇ for supporting and encouraging me with their best wishes.

Special thanks to Eda ADAL and Taner İNCE for their kind help and encouragement.

Finally, I wish to thank my parents, Edibe DEMİR and Ali DEMİR for their kind support and patience at every stages of this study.

TABLE OF CONTENTS

ABSTRACT	V
ÖZET	VI
ACKNOWLEDGEMENTS	VIII
TABLE OF CONTENTS	IX
LIST OF FIGURES	XI
LIST OF TABLES	XIII
LIST OF SYMBOLS/ABBREVIATIONS	XIV
CHAPTER I (INTRODUCTION)	1
1.1. Insulation Coordination and Impulse Voltages	1
1.2. Breakdown Characteristics of Impulse Voltage Test	6
1.3. Method of Determining 50% Breakdown Voltage.....	9
1.3.1 Multiple-Level Tests	9
1.3.2 Successive Discharge Tests	10
1.3.3 Up-and-Down Tests	10
1.4. Unaccuracy in Up-and-Down Test.....	11
CHAPTER II (STATISTICAL INVESTIGATION OF BREAKDOWN PHENOMENA)	13
2.1 Introduction	13
2.2 Effects of Sweep Voltages to Statistical Time-Lag and Breakdown	14
2.3 Determining the distribution function of impulse breakdown voltage.....	16
2.4 Maximum Likelihood Estimation (MLE)	18
2.4.1 Maximum Likelihood Estimation of Normal Distribution	19
2.4.2 Maximum Likelihood Estimation of Logistic Distribution	20
2.4.3 Maximum Likelihood Estimation of Three-Parameter Weibull Distribution	20
2.4.4 Maximum Likelihood Estimation of Gumbel Distribution.....	21
2.5 Goodness-of-Fit Procedure.....	22
2.5.1 Kolmogorov-Smirnov Goodness-of-Fit Test.....	22

2.5.2	Likelihood Ratio Test.....	23
2.5.3	Quantile-Quantile Plots.....	24
CHAPTER III	(EXPERIMENTAL SETUP).....	25
3.1	Two-Stage Swing-Motion Impulse Generator	25
3.2	Experimental Setup of External DC Sweep Voltage.....	25
CHAPTER IV	(RESULTS AND DISCUSSIONS).....	29
4.1	Up-and-Down Breakdown Test Data	29
4.2	Results of Parameter Estimates	33
4.3	Discussion of Kolmogorov-Smirnov Test Results	36
4.4	Discussion of Likelihood Ratio Test Results	37
4.5	Discussion of Quantile-Quantile Plots	39
4.6	Logistic Plots of Various Sweep Voltages Data and Confidence Limits....	45
4.7	Experimental Time-Lag Results.....	50
CHAPTER V	(CONCLUSION)	56
REFERENCES	58
APPENDICES	61
A.1	Numerical Solution of Log-Likelihood Equations	61
A.1.1	Main Algorithm for Newton-Raphson Method.....	63
A.2	Monte Carlo Optimization of Log-likelihood Equations	64
A.2.1	Main Algorithm for Monte Carlo Optimization Method.....	65
A.3	Generation of Impulse Voltages.....	66
A.3.1	Impulse Voltage Generator Circuits.....	66
A.3.1.1	Single-Stage Impulse Generator Circuits	67
A.4	Normalization of Up-and-down Test Data to STP Conditions	69

LIST OF FIGURES

Figure 1.1 Full lightning impulse voltage without any oscillations or overshoots.	2
Figure 1.2 Examples of lightning impulse voltages with oscillations and overshoots.	3
Figure 1.3 Lightning impulse voltage chopped on the tail.....	4
Figure 1.4 Voltage-time curve for impulses of constant prospective shape.	5
Figure 1.5 Full switching impulse.....	5
Figure 1.6 Breakdown probability curve.....	7
Figure 1.7 Breakdown and withstand probability curves.....	8
Figure 1.8 An example of a typical insulation co-ordination system.....	9
Figure 2.1 (a) Definition of critical volume and (b) its dependence on applied gap voltage.	14
Figure 3.1 Two-stage swing-motion impulse generator.	26
Figure 3.2 Impulse generator used in the experiments and rod-plane test gap.	27
Figure 3.3 Lightning impulse voltage waveshape obtained from swing-motion impulse generator.	28
Figure 3.4 Experimental setup and sweep voltage deterring sphere-to-sphere gap.	28
Figure 4.1 Up-and-down test data for positive sweep voltages. 50% impulse breakdown voltages are indicated.	31
Figure 4.2 Up-and-down test data for negative sweep voltages. 50% impulse breakdown voltages are indicated.	33
Figure 4.3 Q-Q plots of four distributions for 0 V sweep voltage data.	40
Figure 4.4 Q-Q plots of four distributions for + 75 V sweep voltage data.	41
Figure 4.5 Q-Q plots of four distributions for + 150 V sweep voltage data.	41
Figure 4.6 Q-Q plots of four distributions for + 300 V sweep voltage data.	42
Figure 4.7 Q-Q plots of four distributions for 0 V sweep voltage data.....	43
Figure 4.8 Q-Q plots of four distributions for - 75 V sweep voltage data.	43
Figure 4.9 Q-Q plots of four distributions for - 150 V sweep voltage data.	44
Figure 4.10 Q-Q plots of four distributions for – 300 V sweep voltage data.....	44

Figure 4.11 Logistic plot of 0 V sweep voltage data and 95% confidence limits.....	45
Figure 4.12 Logistic plot of + 75 V sweep voltage data and 95% confidence limits.	46
Figure 4.13 Logistic plot of + 150 V sweep voltage data and 95% confidence limits.	46
Figure 4.14 Logistic plot of + 300 V sweep voltage data and 95% confidence limits.	47
Figure 4.15 Logistic plot of 0 V sweep voltage data and 95% confidence limits.....	47
Figure 4.16 Logistic plot of - 75 V sweep voltage data and 95% confidence limits.	48
Figure 4.17 Logistic plot of - 150 V sweep voltage data and 95% confidence limits.	48
Figure 4.18 Logistic plot of - 300 V sweep voltage data and 95% confidence limits.	49
Figure 4. 19 Histograms of statistical time-lag data for various positive sweep voltages.....	50
Figure 4. 20 Histograms of statistical time-lag data for various negative sweep voltages.....	51
Figure 4.21 Laue plots for the rod-plane test gap for various positive sweep voltages.	53
Figure 4.22 Laue plots for the rod-plane test gap for various negative sweep voltage.	54
Figure A.1 Flow chart of Newton-Raphson Method.....	64
Figure A.2 Flow chart of Monte Carlo Optimization.....	66
Figure A.3 Single-stage impulse generator circuits.	68

LIST OF TABLES

Table 4. 1 Positive sweep voltages and STP normalized impulse up-and-down test results	30
Table 4. 2 Negative sweep voltages and STP normalized impulse up-and-down test results	32
Table 4. 3 Maximum likelihood estimates for <u>positive</u> sweep voltage data.	34
Table 4. 4 Maximum likelihood estimates for <u>negative</u> sweep voltage data.....	35
Table 4. 5 Kolmogorov Smirnov test results for positive sweep voltage data.	36
Table 4. 6 Kolmogorov Smirnov test results for negative sweep voltage data.	37
Table 4. 7 Likelihood ratio test results for positive sweep voltage data.	38
Table 4. 8 Likelihood ratio test results for negative sweep voltage data.	39

LIST OF SYMBOLS/ABBREVIATIONS

LI	Lightning Impulse
SI	Switching Impulse
EHV	Extra High Voltage
3PW	Three-parameter Weibull
cdf	Cumulative Distribution Function
pdf	Probability Density Function
MLE	Maximum Likelihood Estimation
LL	Log-likelihood
K-S	Kolmogorov-Smirnov
LR	Likelihood Ratio
Q-Q	Quantile-Quantile
STP	Standard Temperature and Pressure
RAH	Relative Air Humidity
N-R	Newton-Raphson
MC	Monte Carlo

CHAPTER I

INTRODUCTION

1.1. Insulation Coordination and Impulse Voltages

The term “insulation coordination” means that arrangement of insulation levels of power equipments against any insulation failure in the electric power system. Insulation coordination is important for keeping interruptions minimum and allows continuous operation of electric power grid in the case of any insulation outages.

In electric grids, nominal voltages of power equipments are determined optimally, and they may sometimes increase above their rated values. These overvoltages are called “maximum system voltage”. Maximum system voltages are allowed to exist in a very short duration.

There are two types of impulse voltages; lightning and switching impulses. A lightning impulse is generated on power lines when a lightning strikes on or near transmission lines. Switching impulse voltage is usually formed due to switching of circuit breakers during power grid operation.

To achieve an optimum and continuous operation of power grid, and to determine variation of insulation level is quite important. We can classify the insulation levels in two situations; below 300 kV and above 300 kV. If the voltage rating of the power equipment is less than 300 kV, insulation level is a statement of lightning impulse withstand voltage. If the voltage rating of the power equipment is greater than 300 kV, insulation level is a statement of switching impulse withstand voltage [1].

Lightning Impulse (LI) Voltage:

As shown in Figure 1.1, the waveshape is known as, $T_1/T_2 = 1.2/50 \mu s$ wave, T_1 is the virtual rising time and T_2 is the virtual time to half-value. T_1 is obtained multiplying T by 1.67, where T is the time interval between the instants when the impulse has 30% and 90% of the peak value, these instants correspond to points A and B. T_2 is the time interval between the virtual origin (O_1) and the instant on the tail when the voltage has decreased to half of the peak value. Virtual origin (O_1) is the intersection point with the time axis of a straight line drawn through points A and B on the front of LI waveform, and virtual origin O_1 precedes by a $0.3 \cdot T_1$ from the instant that corresponds to the point A.

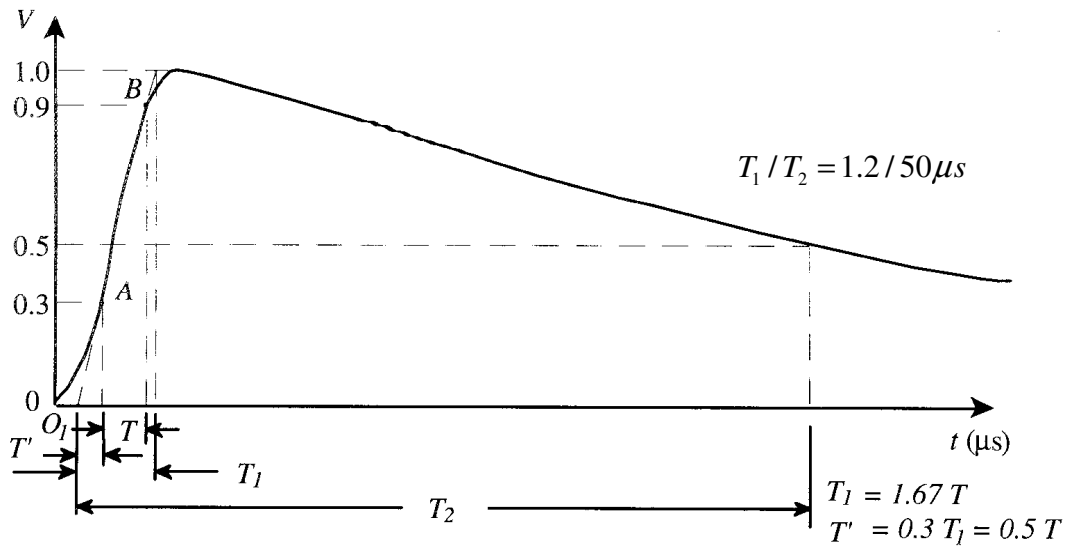


Figure 1.1 Full lightning impulse voltage without any oscillations or overshoots.

In practice, LIs have some overshoots and oscillations. It is very hard to produce LI that has no overshoot and oscillation in laboratory conditions. The value of the test voltage for a LI without any overshoot or oscillations is its peak value. Some LIs that have overshoots and oscillations are shown in Figure 1.2. To determine the peak value of LI including overshoots and oscillations is difficult. When overshoots and oscillations occurred, determination of peak value of LI depends on oscillation frequency and overshoot duration. If the oscillation frequency is less than 0.5 MHz or greater than 1 μs , the peak value is accepted as the maximum value of the waveform. If the oscillation frequency is greater than 0.5 MHz or less than 1 μs , the

peak value is determined from the maximum value of the mean curve. In Figures 1.2 (a) and (b), the value of test voltage is calculated by a mean curve. In Figures 1.2 (c) and (d), the value of test voltage is determined by the peak value. In Figures 1.2 (e), (f), (g) and (h), no guidance can be given to determine the value of test voltage.

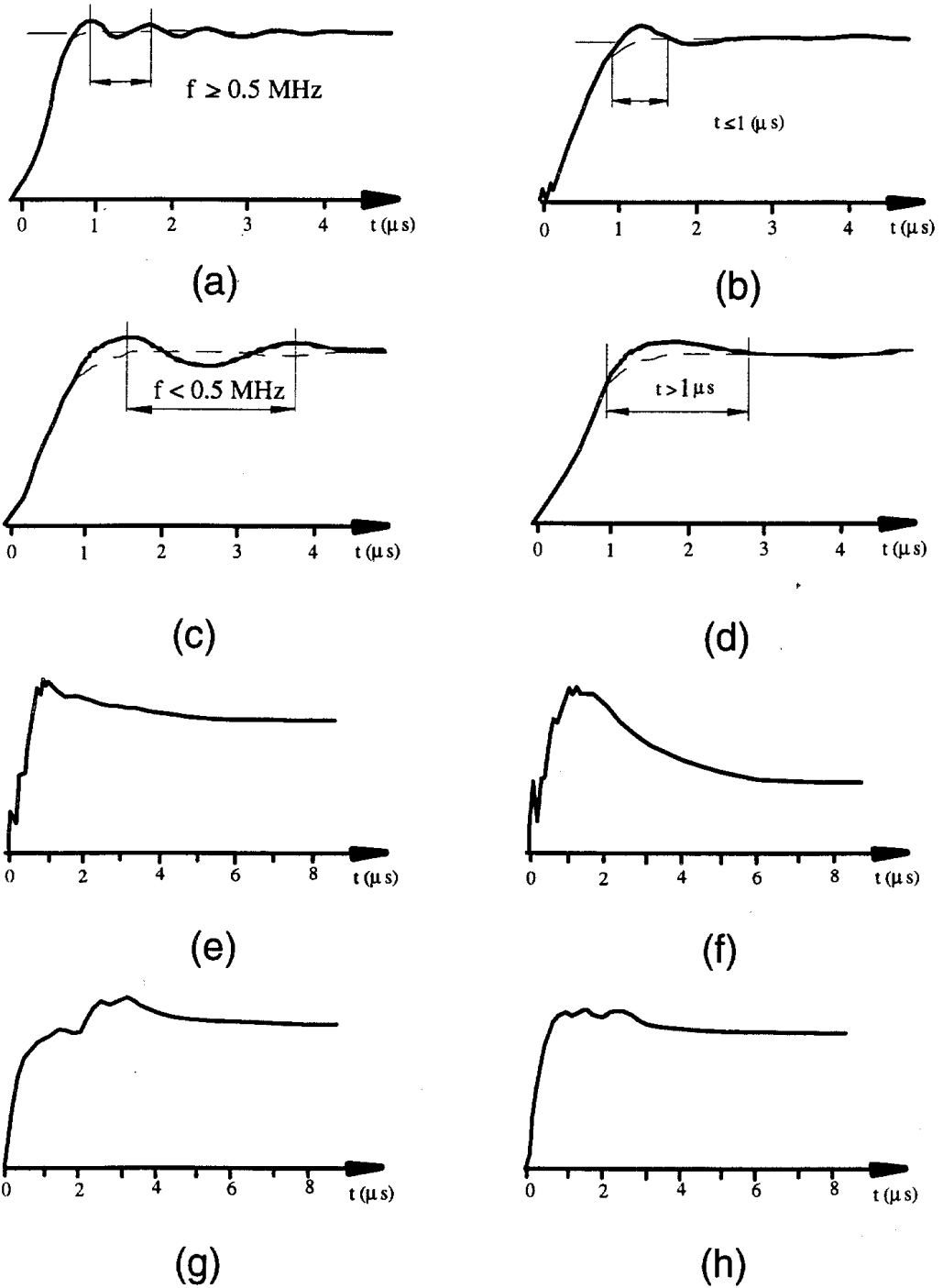
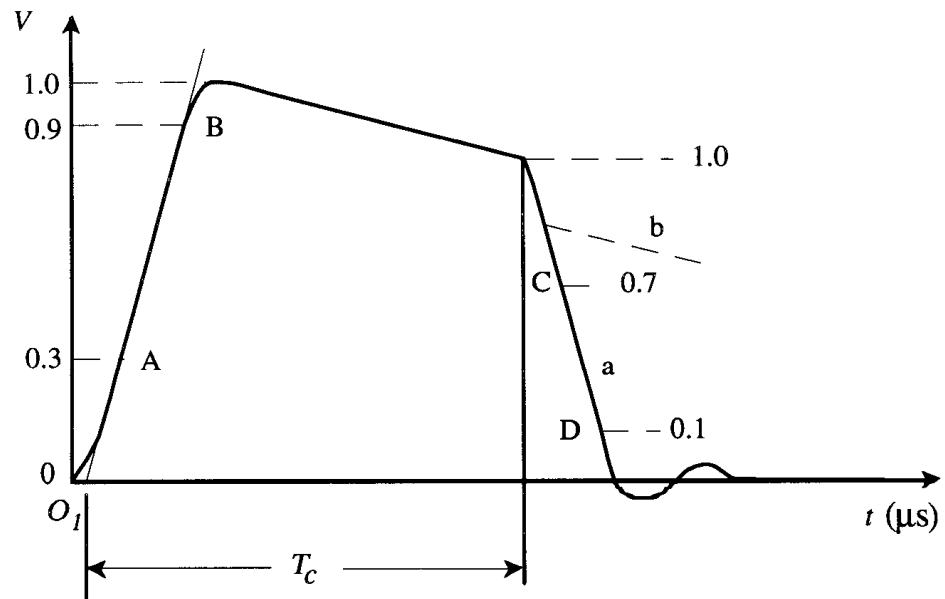


Figure 1.2 Examples of lightning impulse voltages with oscillations and overshoots.

A chopped lightning impulse is formed when any type of discharge causes a rapid collapse of the voltage. The discharge that causes collapse of voltage, may occur due to internal or external insulation failure of a test object. The time to chopping (T_c) is the time interval between the virtual origin (O_1) and the instant of chopping. A chopped lightning impulse waveform collapsed at the tail is shown in Figure 1.3.



- a—Chopped wave caused by a disruptive discharge.
- b—Chopped wave caused by a nondisruptive discharge.

Figure 1.3 Lightning impulse voltage chopped on the tail.

On the tail part of the chopped waveform, the intersection of 10%-70% line (line CD) with the waveform and time axis determines the voltage at the instant of chopping and therefore the chopping time T_c [2].

The voltage/time curve shown in Figure 1.4 indicates different chopping phases on the LI waveforms; on the front , at the peak or on the tail. When the peak value of applied LI is decreased , the chopping time of LI increases. The voltage/time curve which passes through the voltage points where choppings occurred determines basic insulation level to which the power equipment should withstand.[3].

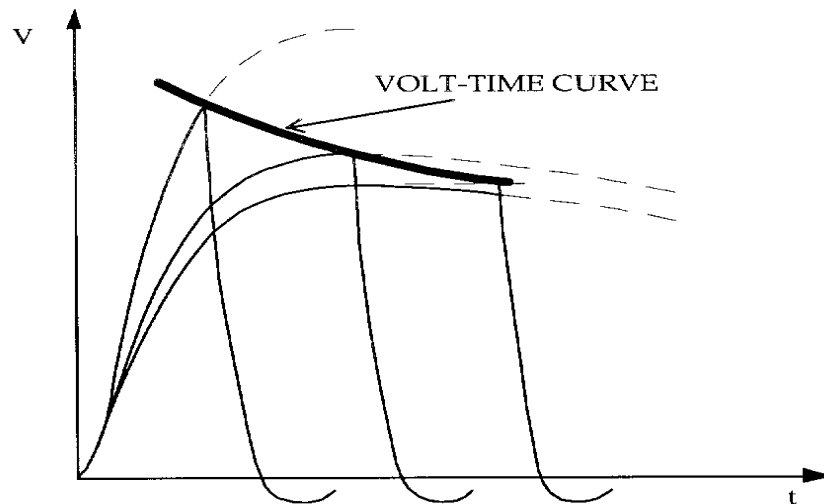


Figure 1.4 Voltage-time curve for impulses of constant prospective shape.

Switching Impulse (SI) Voltage:

The standard switching impulse voltage known as $T_p / T_2 = 250 / 2500 \mu s$ where T_p is the rising time to peak and T_2 is the decaying time to half-value. The waveform of SI is shown in Figure 1.5. T_1 is the time interval between the instants when the voltage has values 90% of its peak.

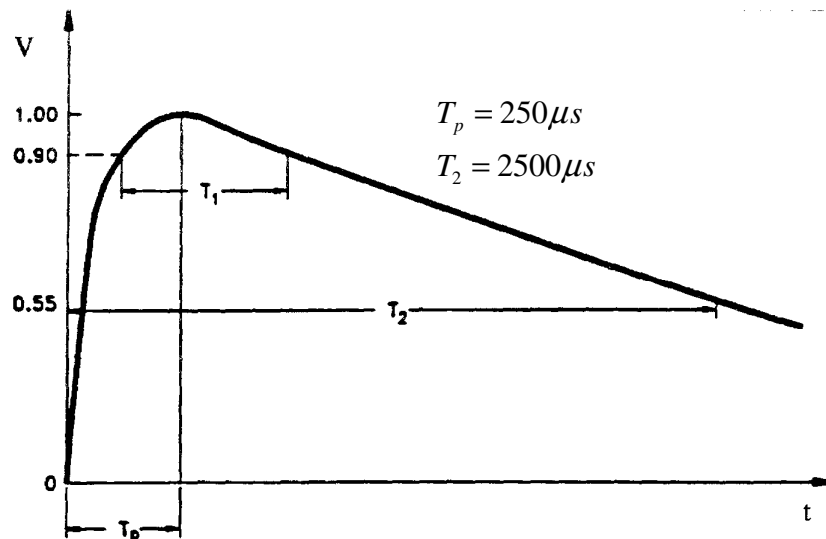


Figure 1.5 Full switching impulse.

Peak values of LI and SI voltages are critical in determining withstand voltage in relation to basic insulation level of a power transmission and distribution networks [2].

1.2 Breakdown Characteristics of Impulse Voltage Test

The results taken from many laboratory tests with impulse voltages show that breakdown voltage has statistical characteristic: The probability of breakdown changes according to peak value of applied impulse voltage and depends on many known and unknown physical factors.

The probability of breakdown under impulsive fields is of great importance. There are two basic processes of concern in occurrence of breakdown. First one is the appearance of avalanche-initiating electrons and the second one is the temporal growth of current after all conditions that cause breakdown are satisfied.

Natural sources may not be adequate to produce an initiating electron when the impulse is applied because of the short duration of applied impulse waveform (approximately microseconds level). It is important to note that finding an initiatory electron in the gap is statistically distributed. The time t_s which elapses between the application of a impulse voltage to the spark gap and the appearance of initiatory electron is called the statistical time lag. After the appearance of free electron, the time t_f required for the ionization processes to produce a current which has a sufficient magnitude is formative time lag.

In the statistical time lag, two probabilities play a key role, P_1 is the probability of an appearance of an electron in the gap which can lead to breakdown. Since it is not known that whether such an electron can cause to a breakdown or not, causing to breakdown of such an electron is also probabilistic and its value is P_2 . Basically, probability of breakdown (P) is equal to P_1P_2 , and the average statistical time lag is $1/\beta P_1P_2$, where β represents effects of peripheral factors like the level of surrounding irradiation, and the surface condition of cathode material.

It is generally assumed that breakdown probability curve has a good resemblance to the cumulative normal distribution function which is shown in Fig.1.6, we can divide breakdown probability curve into three different zones; Zone1, Zone2, and Zone3. Zone1 shows the probabilities of voltages which are smaller than the highest withstand voltage (V_A). Zone2 shows the probabilities of voltages which are between

the highest withstand voltage (V_A) and the lowest breakdown voltage (V_B). 50% breakdown voltage lies in Zone2. Zone 3 shows the probabilities of voltages which are greater than the lowest breakdown voltage (V_B). The probability values are close to 0 in Zone1 and the probability values in Zone3 are near to 1.

Even if we know that breakdown probability curve $P = P(V)$ obviously exists, it is not possible to determine it exactly by means of measurements. This is caused by the fact that the curve has to be found by using statistical estimation techniques, deviations in the results therefore cannot be avoided. The size of these deviations depends on the number of applied impulses, provided all other influencing factors are kept constant. The breakdown probability curve is fully determined by two parameters V_{50} and σ . In this curve, 0% probability is at $-\infty$, and 100% probability is at $+\infty$. That's why the breakdown probability curve does not exist in the finite range. The 50% breakdown voltage is the characteristic value for EHV equipment, because this value is relatively simple to determine with sufficient accuracy and should be provided by manufacturer for the usage of the installer. There are several methods of measurement suitable for a determination of the 50% value. Three of these methods are described in [2]. The 50% breakdown voltage cannot be used directly in insulation coordination, where the voltages near to 0% and 100% probability are the voltages of real importance.

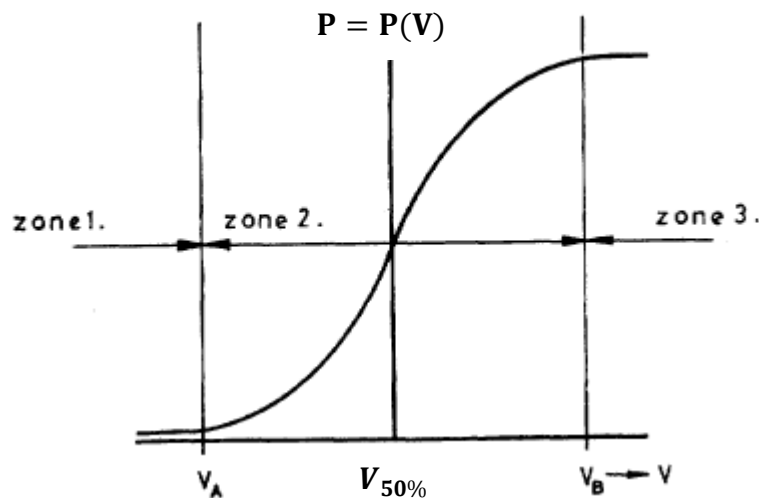


Figure 1.6 Breakdown probability curve.

There are three important parameters on the breakdown probability curve which are used to determine the level of insulation coordination (Figure 1.6). They are:

- 1) The highest withstand voltage V_A .
- 2) The 50% breakdown voltage that corresponds to a probability of 0.5 on breakdown probability curve.
- 3) The lowest breakdown voltage V_B .

As shown in Figure 1.7, statistical impulse withstand voltage probability is characterized by two distinct curves: breakdown probability and withstand probability curves. Statistical impulse withstand voltage of any insulation system is the peak value of a SI or LI test voltage at which insulation can withstand. To designate the withstand voltage of power equipments in insulation coordination, a voltage, which corresponds to a 10% probability on the breakdown probability graph, is selected. 10% impulse voltage corresponds to a 90% probability voltage on the withstand probability plot.

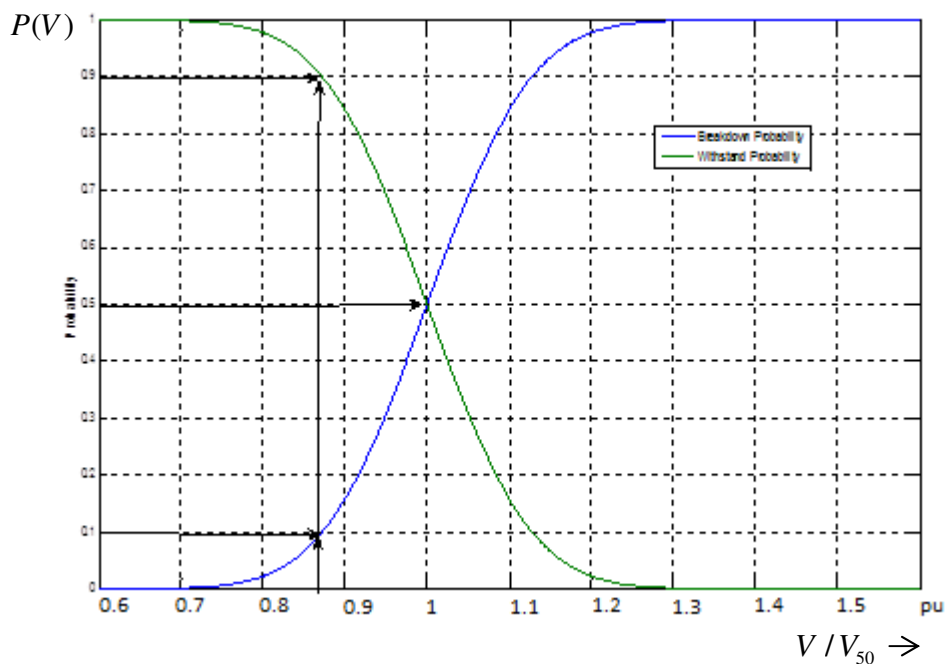


Figure 1.7 Breakdown and withstand probability curves

50 % impulse breakdown voltage and standard deviation σ value plays a key role in determining probability function of breakdown [4,5].

In order to avoid insulation failure, the insulation level of different types of equipment connected to the system has to be higher than the magnitude of highest transient overvoltages that appear on the system. The magnitude of transient overvoltages are usually limited to a protective level by protective devices. Thus the insulation level has to be above the protective level by a safe margin (Figure 1.8). Normally, the impulse insulation level is established at a value 15-25% above the protective level [1].

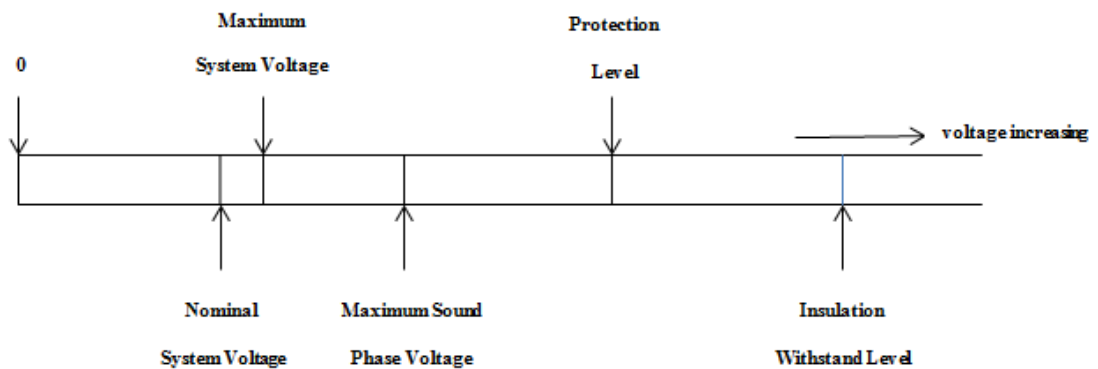


Figure 1.8 An example of a typical insulation co-ordination system

1.3 Method of Determining 50% Breakdown Voltage

To determine 50% breakdown voltage (V_{50}) and standard deviation (σ), some breakdown tests in uniform, quasi-uniform and non-uniform field gaps are performed. These tests can be divided into three categories.

- 1) Multiple-level tests
- 2) Successive discharge tests
- 3) Up-and-down tests

1.3.1 Multiple-Level Tests

In multiple-level tests, for every voltage levels selected as $V_i (i=1,2,\dots,n)$ and m_i substantially equal voltage stresses (e.g. LIs) are applied at each voltage level V_i . This method is generally applied at impulse voltage tests but some tests with alternating and direct voltage tests also fall into this class.

The tests result in d_i number of breakdown voltages for m_i numbers of voltages applied across the test gap at each voltage level V_i [2].

1.3.2 Successive Discharge Tests

In successive discharge tests, the procedure leading to determine the breakdown voltage of a test object follows application of n number of successive voltages to the test gap. The test voltage may be increased continuously until a breakdown occurs, or the test voltage may be held constant at some level until a breakdown is observed. The results are the n values of voltage V_i (or time t_i) at which the breakdown occurred.

Such tests are made with direct, alternating, or impulse voltages. Tests where disruptive discharges occur on the front of the impulse fall into this class [2].

1.3.3 Up-and-Down Tests

Up-and-down method is the test procedure used to estimate 50% probability breakdown voltage. This recognition of 50% probability breakdown voltage is the result of approximation to assumed normal probability distribution of the test results. For an initial chosen voltage value V_k which is thought to be approximately equal to the 50% breakdown voltage level is applied across the test gap. An impulse is applied at the level V_k . If this does not cause a breakdown, the next impulse should have the level $V_k + \Delta V$ where a voltage interval ΔV , approximately 3% of V_k , is chosen. If a breakdown occurs at the level V_k , the next impulse should have the level $V_k - \Delta V$.

This procedure is continued, the level of each impulse being thus determined by the result of the previous one, until a sufficient number of observations has been recorded. The number of impulses n_i applied at each level V_i is then counted and the 50% disruptive discharge voltage is given by:

$$V_{50\%} = \frac{\sum n_i V_i}{\sum n_i} \quad (1.1)$$

n_i should be greater than 20 for higher accuracies. The higher number of voltages are applied, the more accurate 50% impulse breakdown voltage is obtained [6].

1.4 Unaccuracy in Up-and-Down Test

In order to design insulation systems, it is essential to assess the breakdown probability of the various air gaps and recovery-type insulation systems. Up-and-Down method is used to estimate 50% probability breakdown voltage and standard deviation σ (scaling parameter). But there are doubts whether these estimates are reliable or not [5].

Estimation of breakdown voltages corresponding to low probability fractiles which are important for determining basic insulation level of power equipment that requires precise knowledge of V_{50} and σ . In fact, it is also important to know that a certain error in σ may increase error in the estimation of low probability fractiles [5].

The classical up-and-down method of Dixon and Mood was based on a maximum likelihood estimation of V_{50} and σ for a normal distribution. However, due to the lack of modern computing facilities at that time, Dixon and Mood developed a simple approximation to the maximum likelihood estimator [5]. In order to obtain the exact values of V_{50} (μ) and σ , maximum likelihood method is widely used.

In classical up-and-down method, LI or SI voltages are applied specified number of times. It is assumed that breakdown probability distribution is normally distributed in classical Up-and-Down method. Up-and-down method is particularly effective for estimating the mean voltage value. It is not a good method for estimating small or large probability fractiles unless normality of the distribution is assured. The interval between testing levels should be approximately equal to the standard deviation. In any experiment the total number of successes will be approximately equal to the total number of failures. We shall let N denote the smaller total and let $n_0, n_1, n_2, \dots, n_k$

denote the frequencies at each voltage level for this less frequent event where n_0 corresponds to the lowest level and n_k the highest level on which the event occurs. We have then $\sum n_i = N$ [7].

The estimates of μ and σ are based on the first two moments of the voltage values using the frequencies n_i . But since the voltage values are equally spaced, the moments are more easily computed in terms of the two sums

$$A = \sum in_i \quad (1.2)$$

$$B = \sum i^2 n_i \quad (1.3)$$

We estimate the value of $V_{50\%}$ and σ using the following two equations.

$$V_{50\%} = v' + d \left(\frac{A}{N} \pm \frac{1}{2} \right) \quad (1.4)$$

Here the plus sign is taken when the nonbreakdown number is used and the minus sign in the opposite case; v' is the voltage corresponding to $i=0$ [7,8]. This equation (1.4) gives the same result with the previous equation (1.1) that is used for estimating $V_{50\%}$.

$$s = 1.62d \left(\frac{NB - A^2}{N^2} + 0.029 \right) \quad (1.5)$$

This equation is used for estimating standard deviation (σ) value. d is the voltage interval between two successive voltage applications in up-and-down method [7,8].

CHAPTER II

STATISTICAL INVESTIGATION OF BREAKDOWN PHENOMENA

2.1 Introduction

There are two conditions which must be simultaneously satisfied in order that an impulse discharge can occur in air. First, there should be at least one suitably located free electron in air, and secondly, the electric field should be of sufficiently high within the critical volume (see definition of critical volume) of the stressed electrode to ensure that this electron produces a sequence of avalanches which lead to breakdown. In the absence of an initiatory electron in this volume, no single avalanche can lead to breakdown even if the electric field exceeds the breakdown field strength of the gas medium [9].

Free electrons are produced naturally in the air as a result of external radiation due to cosmic rays and the penetration of ultraviolet radiation from the sun or the presence of local radioactive materials. Once an electron is liberated, it is attached to an electronegative oxygen molecule rapidly and removed effectively. Indeed, the rate of production and concentration of free electrons are quite random. When an overvoltage impulse is applied to a spark gap in air, there is only a small probability of there being a liberated electron between two electrodes. Some time elapses are needed before breakdown to occur [9].

Definition of critical volume: At the tip and around any stressed electrode in gases, a volume is determined between two boundaries: $\bar{\alpha} = 0$ and $\int \bar{\alpha} dr = \ln N_{cr}$ which is known as 'critical volume' where $\bar{\alpha}$ is the effective ionization constant and N_{cr} is the critical electron concentration in an avalanche giving rise to an initiation of a streamer. The limits of integration is determined by the geometric parameters of the gap related to generation of N_{cr} . Ionization occurs in any gas effectively when an

initiatory electron appears within the critical volume closer to the stressed electrode surface (Figure 2.1).

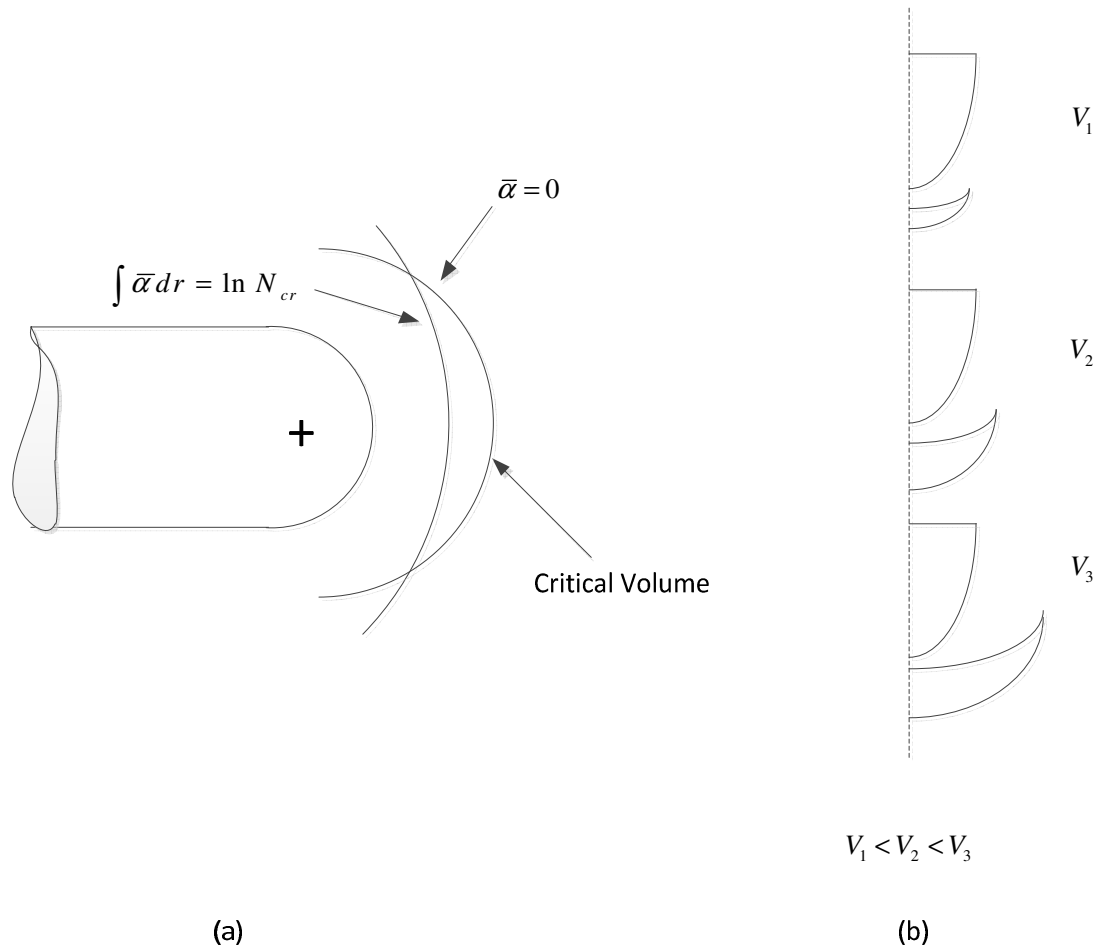


Figure 2.1 (a) Definition of critical volume and (b) its dependence on applied gap voltage.

Since the distributions of free electrons close to the stressed electrode is statistical in nature, their distribution should be known before any laboratory and field tests performed on high voltage power equipment. Since the concentration of free electrons and their probability of occurrence in the critical volume is undeterministic, there is no definitive method that is applied for determining breakdown voltage under LI&SI stresses. If the applied voltage on test gap is increased, the critical volume becomes larger as shown in Figure 2.1(b).

2.2 Effects of Sweep Voltages to Statistical Time-Lag and Breakdown

It is thought that the breakdown probability and statistical time-lag in air and other electronegative gases can be correlated directly with the density of the small negative

ions. There should exist a correlation between the statistical time-lag distribution and the initial spatial ion densities [10].

This correlation can be presented with the relationship between the time-lag distribution and the rate of production of initiating electrons, $k(t)$, is given by the Laue expression [10],

$$\bar{P}(t) = \exp\left(-\int_0^t \beta k(t) dt\right) \quad (2.1)$$

where β is the probability that an electron will cause breakdown and $\bar{P}(t)$ is the probability that breakdown has not occurred in the time interval $0-t$. It is useful to represent the experimental time-lag results in the form of a ‘Laue plot’ [10].

$$\ln \bar{P}(t) = -\int_0^t \beta k(t) dt \quad (2.2)$$

then the slope of the Laue plot is proportional to the rate of production of initiating electrons [10].

It is assumed that very small electric sweep fields across the test gap can have a drastic effect in reducing the small negative ion population [10]. These sweep fields may arise, for example, from leakage across the capacitors of the impulse generator, the remanence magnetic flux in the core of transformers and dielectric polarization within the insulation systems generated across the terminals of power equipment undergoing tests, or from a difference in contact potential between the test electrodes.

It is assumed that applied sweep voltage also affects the breakdown strength of air and electronegative gases. It is thought that sweep fields are adequate to cause the ions in the region of the tip of the rod electrode to be swept either towards or away from the rod, depending on the polarity [11]. Sweep voltages should reduce negative ion density according to these stated theories. To see the effect of sweep field on the breakdown strength, test gap should be isolated from the main impulse generator

with a small air gap, and negative or positive sweep voltages should be applied to the test gap via a high ohmic resistance

The slopes of the Laue plots should be proportional to the rate of production of free electrons which in turn will be proportional to negative ion density in the region of the electrode tip.

Negative ion density changes according to polarity of the applied impulse voltage and the polarity of sweep voltages [10]. When sweep voltage has an opposite polarity to applied impulse voltage, then the rate of production of free electron may be expressed as $k(t) = A_1 + Bt$ and Laue plot function becomes $\ln \bar{P}(t) = A_1 t + Bt^2 / 2$.

When sweep voltage has the same polarity with the applied impulse voltage, then rate of production of free electron and Laue plot function becomes $k(t) = A_2 - Bt$ and $\ln \bar{P}(t) = A_2 t - Bt^2 / 2$, respectively.

The effect of sweep voltage to ion density can be considered from following expression,

$$\rho(r) = 4N(r^{5/2} - r_o^{5/2}) / (5V_o\mu_o r_o^{1/2}) \quad (2.3)$$

where ρ is the negative ion density, r_o is radius of the tip of the electrode, μ_o is the mobility of negative ions, V_o is the sweep voltage, N is the rate of creation of negative ions in per unit volume and approximately 10 ions / cm^3 [11].

2.3 Determining the distribution function of impulse breakdown voltage

The influence of sweep voltage on impulse breakdown voltage distribution has not been investigated so far. The aim of this work is to determine the probability distribution of impulse breakdown voltage under the effect of positive and negative DC sweep voltage. The selected distribution is very important in designing electrical insulation of high-voltage power equipment.

To estimate the impulse breakdown voltage for electrical insulation which has a self-restoring property such as air, vacuum or SF₆ gas, the up-and-down method by Dixon and Mood [7] is generally used, where the underlying distribution is assumed to be the normal distribution [12]. This method is adopted in electrical insulation test standards such as IEC 60060-2 and IEEE Std 4-1995 where the impulse breakdown voltage is thought to follow the normal distribution [12]. In non-self-restoring electrical insulation systems, the up-and-down method is not used because electrical insulation is not usable after it is broken [13]. Bakken assumed that the lightning and switching impulse voltages are characterized by the normal distribution [4]. Hirose proposed new step-up test method for normal, Weibull and Gumbel distributions in the electrical insulation which does not have a self-restoring [12-14]. Yildirim and Korasli have shown that the three-parameter Weibull (3PW) distribution is found to be the best-suited distribution among the other exponential distributions for compressed-gas insulated systems [15]. Korasli have also shown that the statistical distribution of first ac breakdown field data is to be represented by the 3PW distribution [16]. It is also revealed that the impulse breakdown probability distribution of vacuum interrupters follow Weibull distribution when the breakdown voltage is saturated within the investigated contact gaps 10 to 50 mm [17]. Wibholm and Thyregod assessed four different distribution functions for air insulated systems: Normal, logistic, 3PW and Gumbel distributions [18].

In this work, we compare four distribution functions which are commonly used to represent the impulse breakdown voltage of self-restoring insulation systems: Normal, logistic, 3PW, Gumbel distributions. The cumulative distribution function (cdf) of four distributions under investigation are given by

Normal Distribution: The cdf of normal distribution is denoted by

$$P(v) = \frac{1}{\sigma\sqrt{2\pi}} \int_{-\infty}^v \exp\left[-\frac{(t-\mu)^2}{2\sigma^2}\right] dt \quad (2.4)$$

where μ is the mean value and σ is the standard deviation.

Logistic Distribution: The cdf of logistic distribution is given by

$$P(v) = \frac{1}{1 + \exp[-(v - \mu) / s]} \quad (2.5)$$

where μ is the mean value like in normal distribution and s is the scale parameter.

Three-Parameter Weibull Distribution: The cdf of 3PW distribution has the form

$$P(v) = 1 - \exp\left[-\left(\frac{v - \gamma}{\alpha}\right)^\beta\right] \quad (2.6)$$

where α, β, γ are the scale, shape and location (threshold) parameters, respectively and intervals for α, β, γ are given by

$$0 \leq \gamma \leq v_1 \quad (2.7)$$

$$\alpha, \beta > 0 \quad (2.8)$$

where v_1 is the lowest sample in the ordered breakdown voltage data.

Gumbel Distribution: The cdf of Gumbel distribution is given by

$$P(v) = 1 - \exp\left[-\exp\left(\frac{v - \beta}{\alpha}\right)\right] \quad (2.9)$$

where α, β are scale and location parameters, respectively.

2.4 Maximum Likelihood Estimation (MLE)

For the selection of best-fitted distribution for impulse breakdown voltage data which is obtained from up-and-down test under DC sweep voltage, maximum likelihood estimation (MLE) method is used to find the parameters of four different distributions. The MLE method basically depends on the solution of the likelihood function which is defined as the product of probability density functions of selected

distributions and the parameter estimates that maximize the likelihood function are obtained by numerical methods.

Estimation of parameters of selected distributions has a great importance for the high voltage design engineer. Precise knowledge of parameters of distributions is required to make the prediction of fractiles corresponding to extremely low probabilities, which are of particular importance for the insulation coordination. A certain error in the estimation of distribution parameters may increase the error in finding the low probability fractiles such as 5% or 10% [18]. For this reason, MLE method is used to get exact parameter values for the selected distributions.

2.4.1 Maximum Likelihood Estimation of Normal Distribution

The probability density function (pdf) of normal distribution is given by

$$p(v) = \frac{1}{\sigma\sqrt{2\pi}} e^{-\frac{(v-\mu)^2}{2\sigma^2}} \quad (2.10)$$

The likelihood function L corresponding to n breakdowns occurring at each voltage level v_i is denoted by

$$L(v_1, v_2, \dots, v_n | \mu, \sigma) = \prod_{i=1}^n \left[\frac{1}{\sigma\sqrt{2\pi}} e^{-\frac{(v_i-\mu)^2}{2\sigma^2}} \right] \quad (2.11)$$

Since v_i and size n are known, L is a function of μ and σ only. For complete impulse breakdown voltage samples, natural logarithm of the likelihood function

$$\ln L = -\frac{n}{2} \ln(2\pi) - n \ln(\sigma) - \frac{1}{2} \sum_{i=1}^n \left(\frac{v_i - \mu}{\sigma} \right)^2 \quad (2.12)$$

yield the log-likelihood (LL) functions

$$\frac{\partial \ln L}{\partial \mu} = \frac{1}{\sigma^2} \sum_{i=1}^n (v_i - \mu) = 0 \quad (2.13)$$

$$\frac{\partial \ln L}{\partial \sigma} = -\frac{n}{\sigma} + \frac{1}{\sigma^3} \sum_{i=1}^n (v_i - \mu)^2 = 0 \quad (2.14)$$

2.4.2 Maximum Likelihood Estimation of Logistic Distribution

The pdf of logistic distribution is given by

$$p(v) = \frac{e^{-(v-\mu)/s}}{s(1+e^{-(v-\mu)/s})^2} \quad (2.15)$$

Likelihood function for logistic distribution is

$$L(v_1, v_2, \dots, v_n | \mu, s) = \prod_{i=1}^n \left[\frac{e^{-(v_i-\mu)/s}}{s(1+e^{-(v_i-\mu)/s})^2} \right] \quad (2.16)$$

where v_1, v_2, \dots, v_n are the impulse breakdown voltages. The logarithm of the likelihood function is defined by

$$\ln L = -\sum_{i=1}^n \left(\frac{v_i - \mu}{s} \right) - \sum_{i=1}^n \ln(s) - 2 \sum_{i=1}^n \ln(1 + e^{-(v_i-\mu)/s}) \quad (2.17)$$

To find the parameters that maximize the LL function, the following MLE equations need to be solved simultaneously.

$$\frac{\partial \ln L}{\partial \mu} = \frac{n}{s} - 2 \sum_{i=1}^n \left(\frac{\frac{1}{\sigma} e^{-(v_i-\mu)/s}}{1 + e^{-(v_i-\mu)/s}} \right) = 0 \quad (2.18)$$

$$\frac{\partial \ln L}{\partial s} = -\frac{n}{s} + \sum_{i=1}^n \frac{(v_i - \mu)}{s^2} - 2 \sum_{i=1}^n \left(\frac{\frac{(v_i - \mu)}{s^2} e^{-(v_i-\mu)/s}}{1 + e^{-(v_i-\mu)/s}} \right) = 0 \quad (2.19)$$

2.4.3 Maximum Likelihood Estimation of Three-Parameter Weibull Distribution

The pdf of 3PW distribution is defined by

$$p(v) = \frac{\beta}{\alpha} \left(\frac{v-\gamma}{\alpha} \right)^{\beta-1} \exp \left[-\left(\frac{v-\gamma}{\alpha} \right)^\beta \right] \quad (2.20)$$

The likelihood function is given by

$$L(v_1, v_2, \dots, v_n | \alpha, \beta, \gamma) = \prod_{i=1}^n \left[\frac{\beta}{\alpha} \left(\frac{v_i - \gamma}{\alpha} \right)^{\beta-1} \exp \left[- \left(\frac{v_i - \gamma}{\alpha} \right)^\beta \right] \right] \quad (2.21)$$

v_1, v_2, \dots, v_n are the lightning impulse breakdown voltages. The logarithm of likelihood function is denoted by

$$\ln L = n \ln \left(\frac{\beta}{\alpha} \right) + (\beta - 1) \sum_{i=1}^n \ln (v_i - \gamma) - \frac{1}{\alpha} \sum_{i=1}^n (v_i - \gamma)^\beta \quad (2.22)$$

LL equations are given by

$$\frac{\partial \ln L}{\partial \alpha} = -\frac{n}{\alpha} + \frac{1}{\alpha^2} \sum_{i=1}^n (v_i - \gamma)^\beta = 0 \quad (2.23)$$

$$\frac{\partial \ln L}{\partial \beta} = \frac{n}{\beta} + \sum_{i=1}^n \ln (v_i - \gamma) - \frac{1}{\alpha} \sum_{i=1}^n \left[(v_i - \gamma)^\beta \ln (v_i - \gamma) \right] = 0 \quad (2.24)$$

$$\frac{\partial \ln L}{\partial \gamma} = \frac{\beta}{\alpha} \sum_{i=1}^n \ln (v_i - \gamma)^{\beta-1} - (\beta - 1) \sum_{i=1}^n (v_i - \gamma)^{-1} = 0 \quad (2.25)$$

2.4.4 Maximum Likelihood Estimation of Gumbel Distribution

The pdf of Gumbel distribution has the form

$$p(v) = \left(\frac{1}{\alpha} \right) \exp \left(\frac{v - \beta}{\alpha} \right) \exp \left[- \exp \left(\frac{v - \beta}{\alpha} \right) \right] \quad (2.26)$$

Likelihood function is given by

$$L(v_1, v_2, \dots, v_n | \alpha, \beta) = \prod_{i=1}^n \left[\left(\frac{1}{\alpha} \right) \exp \left(\frac{v_i - \beta}{\alpha} \right) \exp \left[- \exp \left(\frac{v_i - \beta}{\alpha} \right) \right] \right] \quad (2.27)$$

where v_1, v_2, \dots, v_n are the impulse breakdown voltages obtained from up-and-down test. The logarithm of likelihood function is denoted by

$$\ln L = n \ln \left(\frac{1}{\alpha} \right) + \sum_{i=1}^n \left(\frac{v_i - \beta}{\alpha} \right) - \sum_{i=1}^n \exp \left(\frac{v_i - \beta}{\alpha} \right) \quad (2.28)$$

The first derivatives of LL function w.r.to distribution parameters α and β yield the following two equations

$$\frac{\partial \ln L}{\partial \alpha} = n\alpha - \sum_{i=1}^n \left(\frac{v_i - \beta}{\alpha^2} \right) + \sum_{i=1}^n \left(\frac{v_i - \beta}{\alpha} \right) \exp\left(\frac{v_i - \beta}{\alpha} \right) = 0 \quad (2.29)$$

$$\frac{\partial \ln L}{\partial \beta} = -\frac{n}{\alpha} + \frac{1}{\alpha} \sum_{i=1}^n \exp\left(\frac{v_i - \beta}{\alpha} \right) = 0 \quad (2.30)$$

There is no explicit solution of LL functions, so they need to be solved numerically. Maximum likelihood estimates of four distributions are calculated by Newton-Raphson method, and all parameters of four distributions are considered to be unknown.

2.5 Goodness-of-Fit Procedure

Kolmogorov-Smirnov (K-S) goodness-of-fit and likelihood ratio (LR) tests are applied to decide the best-suited distribution for the present up-and-down test data which are obtained under the effect of DC sweep voltage. K-S test is applied to compare normal, logistic and Gumbel distributions which are of two-parameter type, and logistic and 3PW distributions that have different number of parameters are compared by LR test. LR test is not used to compare two-parameter type distributions because application of LR test is possible when considered distributions have different number of parameters.

2.5.1 Kolmogorov-Smirnov Goodness-of-Fit Test

Analyzing the works of the researchers in the literature, four different types of distributions are considered to decide on the best-fitted distribution for the present up-and-down test data. Among four distributions, normal, logistic and Gumbel distributions which have two parameters are compared by means of Kolmogorov-Smirnov (K-S) goodness-of-fit test. In order to assess the goodness-of-fit of up-and-down test data by K-S test, the hypothesised distribution should be continuous, and this condition of K-S test is satisfied to compare three distributions, all investigated distributions are continuous type distributions.

The K-S test is a one-sample test designed to assess the goodness-of-fit of a data sample to a continuous distribution $F_v(v)$ [19].

Let $S_n(v)$ be the observed empirical cumulative distribution of random impulse voltages, v_1, v_2, \dots, v_n . The up-and-down test data is sorted in increasing order and the values of $S_n(v)$ are calculated by adding successive frequencies of occurrence, k_i/n for each distinct v_i [19]. It is expected to obtain small deviations of $S_n(v)$ from $F_v(v)$. The K-S test uses the largest of these deviations as a goodness-of-fit measure [18].

$$D_n = \max |F_v(v) - S_n(v)|, \quad \text{for each distinct } v_i \quad (2.31)$$

Maximum of these deviations is used as a K-S test value.

2.5.2 Likelihood Ratio Test

Likelihood ratio test provides to compare the goodness-of-fit of two distribution models. LR test benefits from LL values of distributions. For essentially large sample size, LR test statistic is χ_k^2 -distributed where k is the degrees of freedom. The LR test statistic is given by

H₀: Data come from a logistic distribution model

H₁: Data come from a 3PW distribution model

$$\begin{aligned} R &= -2 * \ln \left(\frac{L_L}{L_{3PW}} \right) \\ &= -2 * \ln L_L + 2 * \ln L_{3PW} \end{aligned} \quad (2.32)$$

where $\ln L_L$ and $\ln L_{3PW}$ are LL values of logistic and 3PW distributions, respectively.

If R is greater than $\chi_{k, 0.05}^2$, then H_0 is rejected and H_1 is accepted. Otherwise, H_1 is rejected and H_0 is accepted. All data is considered at 5% significance level for this work.

$$k = (\text{parameter number of 3PW distribution}) - (\text{parameter number of logistic distribution}) \quad (2.33)$$

To test easily whether the data comes from logistic or 3PW distribution models, p (probability value) is given by

$$p = 1 - \chi^2(R, k) \quad (2.34)$$

where R is the value of LR test.

2.5.3 Quantile-Quantile Plots

Quantile-Quantile plot is a graphical technique to check whether or not the up-and-down test data comes from selected distribution model. In this work, theoretical and actual impulse breakdown voltage data are compared where one axis shows actual impulse breakdown voltage data and the other axis denotes theoretical impulse breakdown voltage data. In order to make use of Q-Q plot, empirical cumulative distribution probabilities for each distinct voltage value are used. Theoretical voltages are produced by inverse distribution function $F^{-1}(p)$ where p values are taken from empirical distribution probabilities. If the actual and theoretical data being compared is similar, the points in Q-Q plot will approximately follow the line $y=x$.

CHAPTER III

EXPERIMENTAL SETUP

3.1 Two-Stage Swing-Motion Impulse Generator

In this work, we investigated the standard lightning impulse voltage breakdown characteristics of air-insulated rod-plane gap system under the influence of positive and negative DC sweep voltages. All data was acquired by up-and-down method which was proposed by Dixon and Mood [7]. As shown in Figure 3.1 the impulse generator which was used in the experiments has two stage and is arranged to fire with a specially designed swing-motion stage-gap system. The impulse generator is of two-stage Marx type and each stage voltage can reach to 120 kV. DC stage voltage can be adjusted to desired voltage level manually before to trigger the system and is measured by a digital voltmeter with the aid of a 1/2000 resistive voltage divider. Each stage is equipped with a 0.26 μF polystyrene capacitor, and hence the impulse generator can deliver maximum of 1.872 kJ (Figure 3.1). With the wave front and tail resistance of 540 Ω and 2.5 k Ω the generator produces the standart 1.2/50 μs lightning waveform (Figure 3.2). The impulse generator used in the present work has one distinct faecture is that the column of two spheres make a free swing-motion to trigger the impulse generator for any impulse voltage level. The impulse waveshape is recorded by the digital storage oscilloscope by means of a capacitive voltage divider (voltage ratio $a=1/3500$). The digital oscilloscope is also connected to a PC and any parameter required in the experiment can be measured by the software of the oscilloscope.

3.2 Experimental Setup of External DC Sweep Voltage

As explained in Section 2.2, the density of electronegative ions in the region close to the rod electrode of a rod-plane gap system is affected by any externally generated voltage (sweep voltage). There are two sources of the sweep voltages: One is resulted from the test objects and the other is the impulse generator itself.

While testing any power equipment, say a power transformer, the sweep voltage is generated owing to remanence magnetization in the ferromagnetic material of transformer core and dielectric polarization within insulation materials.

Sweep voltages are also produced by leakage currents from stage capacitors of the impulse generator.

All these external effects cause sweep voltages to appear across terminals of an unenergized power equipment during field tests prior to triggering the generator [10].

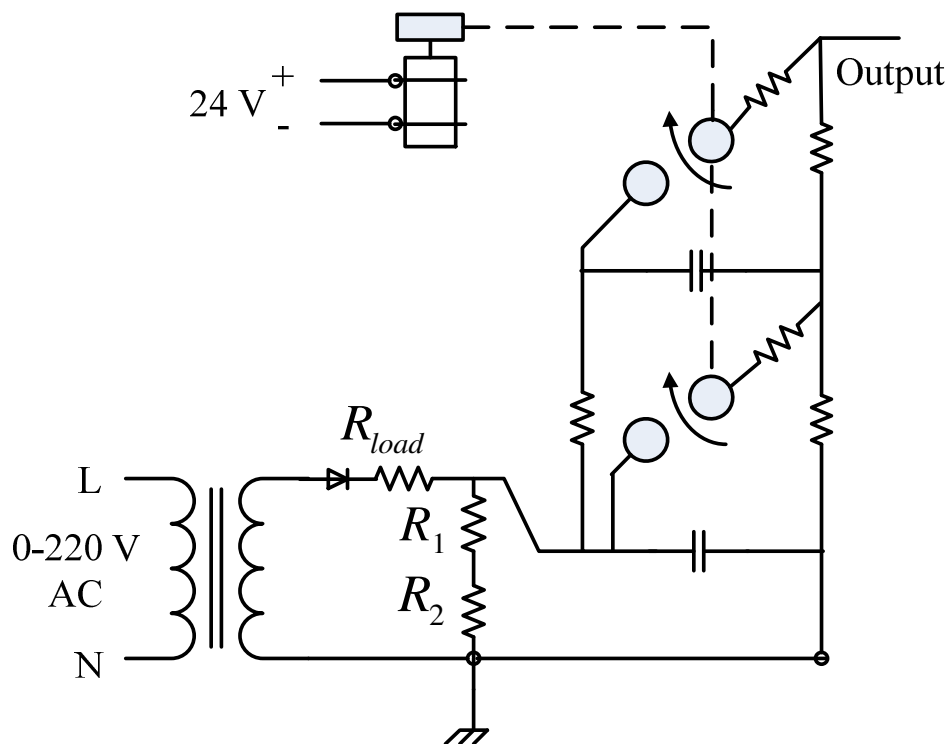


Figure 3.1 Two-stage swing-motion impulse generator.

Sweep voltage was found to affect the insulation strength and statistical time-lag of gas-insulated systems by Somerville and Tedford [10,11], hence, leads to variation of impulse breakdown voltage performance of power equipment undergoing tests. In order to consider the influence of sweep voltage on the impulse breakdown voltage and on the type of distribution functions, a DC voltage source was connected to the test gap via a small sphere-to-sphere gap (Figure 3.3) to isolate the generator from the test gap. The isolator spheres are 2-cm in diameter and was located 1 m away

from the impulse generator. The isolation of the DC source from the impulse generator is done by a $50\text{ M}\Omega$ resistance.



Figure 3. 2 Impulse generator used in the experiments and rod-plane test gap.

During the tests, a rod-plane test gap was used. The height of test gap is 84 cm from the ground level. The rod is 2.5-cm in diameter. The radius of the rod tip is 1 cm and the diameter of the plane is 31.5 cm. The rod-plane test gap can be adjusted manually up to desired length through a gap space adjuster. The rod-plane test gap was set to 3-cm during the tests.

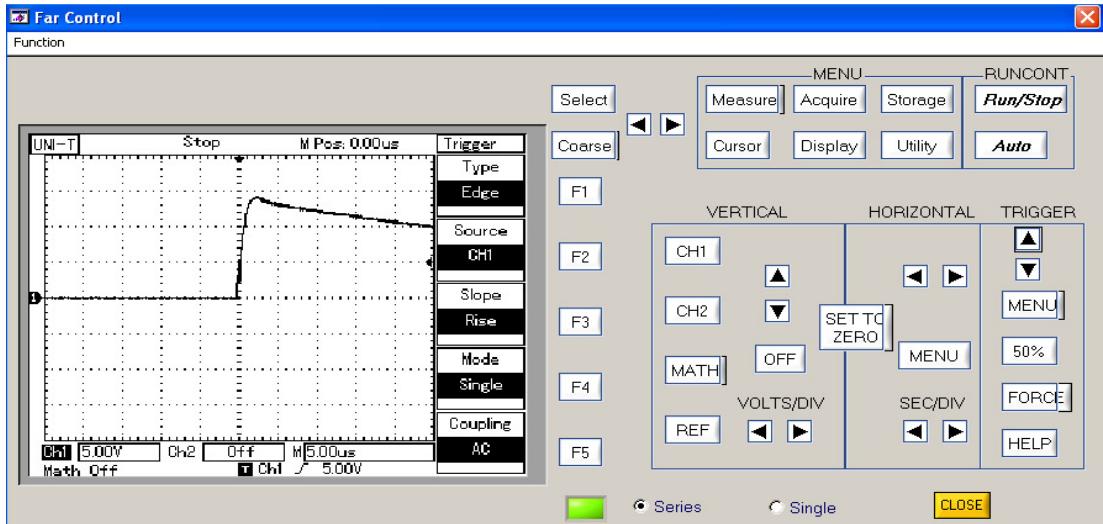


Figure 3. 3 Lightning impulse voltage waveshape obtained from swing-motion impulse generator.

A positive polarity lightning impulse voltage ($1.2/50 \mu\text{s}$) was applied to the test gap throughout the tests. The tests were carried out by up-and-down method [17] and the incremental voltage ΔV was selected as $\sim 1 \text{ kV}$. The occurrence of breakdown was observed from records of the digital storage oscilloscope. The time-lags and peak values were measured from the digital records of oscilloscope via a capacitive voltage divider ($1/3500$). The tests were performed without any interruption to avoid undesirable environmental conditions on the test results.

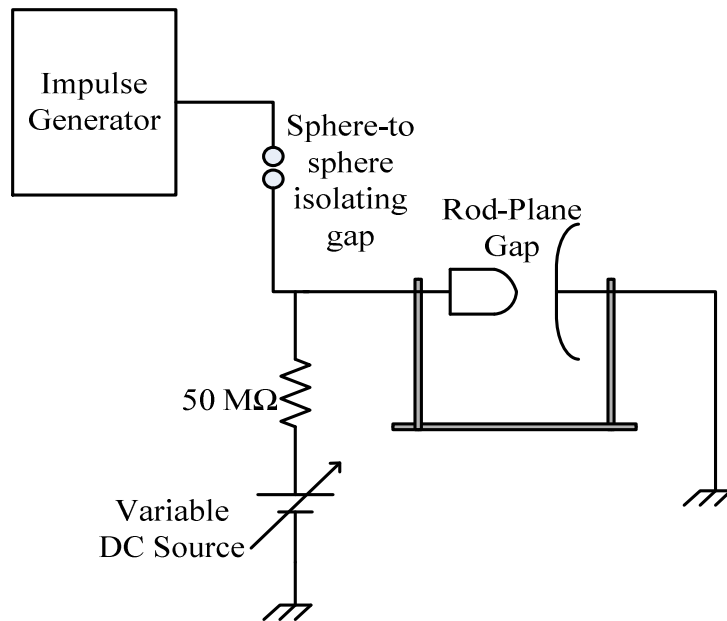


Figure 3. 4 Experimental setup and sweep voltage deterring sphere-to-sphere gap.

CHAPTER IV

RESULTS AND DISCUSSIONS

4.1 Up-and-Down Breakdown Test Data

Up-and-down test data which was obtained under positive and negative sweep voltages are illustrated in Figures 4.1 and 4.2. Number of voltages applied for any set of up-and-down experiment conditions is selected to be as 150 in order to reduce standard deviations with respect to the selected incremental voltage steps and to achieve accurate 50% voltage values. This further allows to optimize the number of voltage applications. Moreover, the tests are performed under strictly similar ambient conditions and impulse breakdown voltages are corrected to STP conditions (see Appendix A.4).

In Table 4.1 normalized up-and-down test data obtained for positive sweep voltages 0 V, +75 V, +150 V, and +300 V are illustrated and the results are plotted in Figure 4.1. Assuming the underlying probability distribution for all up-and-down test data is the logistic type distribution which is the consequence of this study, the 50% impulse breakdown voltage values determined by MLE method are also given in Figures 4.1.

Table 4. 1 Positive sweep voltages and STP normalized impulse up-and-down test results

Sweep voltage (V)	Up-and-down test data (kV)
0 V	52.15 52.5 52.85 53.55 54.6 56 57.75 58.8 59.5 59.85 60.2 59.85 60.2 59.5 47.25 59.5 52.5 59.5 59.15 57.75 56 56 55.3 54.25 49.35 52.5 50.75 46.55 49 49.35 49 49.35 49 45.15 49 49 40.6 48.65 49 49.7 51.1 52.5 51.1 49.35 48.65 49.35 50.75 47.95 49 45.5 47.25 44.1 45.15 44.1 45.15 45.85 47.25 42.35 44.8 45.85 45.15 44.45 45.15 45.85 46.2 40.95 47.6 45.5 44.8 45.5 45.85 45.5 47.25 48.3 49 49.7 51.45 47.25 50.75 50.05 51.8 49.35 51.8 49.35 45.15 47.95 49 45.5 47.25 48.65 49 49.7 48.65 48.3 47.25 48.3 49 49.7 51.1 52.5 51.8 50.75 50.4 49.35 51.8 45.85 51.1 49.35 45.15 47.25 49 44.8 46.9 47.6 47.25 48.3 48.65 48.3 49 50.05 49 49.7 51.1 52.5 52.85 53.55 49.7 49.7 52.5 52.15 49.35 52.15 50.05 49 49 47.95 45.5 49 46.2 45.85 38.5 45.5 47.25 47.95 49 50.4 51.8 52.15 49 48.3
+75 V	52.15 51.1 52.15 52.5 52.85 53.9 55.65 56 48.65 55.65 56 55.65 56.35 51.45 54.6 55.65 49.35 56 56.35 57.75 52.85 52.5 55.65 51.45 54.6 55.65 52.85 55.3 56.175 56.7 57.75 59.15 59.5 61.25 61.6 57.75 52.5 59.5 59.85 50.75 57.75 59.5 57.75 54.25 56 57.05 56 52.15 52.85 52.85 47.6 45.85 45.85 49.35 49.7 49.35 50.75 49 50.75 51.8 52.5 49 52.5 51.8 51.45 52.15 52.5 52.15 50.75 47.6 48.65 49 47.95 49 49 49.35 50.75 51.45 48.65 49.35 45.5 49.35 50.05 52.15 52.5 52.85 53.55 55.3 56 56.35 58.1 54.25 57.75 56.7 59.15 52.5 52.15 52.5 52.15 48.65 52.5 46.2 48.65 49 50.75 51.8 52.5 47.25 52.5 53.2 53.55 54.6 56 55.65 56 52.85 52.5 52.85 53.55 52.5 53.2 49.35 45.85 51.8 51.1 50.4 47.95 49 45.85 46.55 46.9 48.3 49 47.6 45.15 45.5 46.2 47.25 47.25 46.55 47.25 47.6 49 49 50.75 49.35 49 49.35 50.05 49.35
+150 V	52.15 42.35 51.8 50.75 49 48.65 49.35 48.65 49 45.85 48.65 48.65 49 45.5 47.25 48.65 43.75 48.65 49 49 45.15 45.85 47.25 45.85 47.25 48.3 49 49.35 51.1 52.5 52.85 53.2 54.25 55.65 56.35 57.75 58.8 59.5 58.1 50.75 49.7 55.65 50.75 50.05 52.85 48.3 52.5 49 49.7 52.15 52.5 48.65 50.4 49 49 49.7 50.75 49.35 49 49 49.35 49 49.35 51.1 52.15 52.5 53.2 50.4 52.5 52.85 51.1 52.5 52.5 49 49.7 50.75 52.15 50.75 49.7 51.1 51.8 49.35 52.15 52.5 52.85 45.5 52.15 52.5 52.15 51.8 47.25 47.25 47.25 47.25 47.6 49 49.7 50.75 52.15 51.1 52.15 52.5 53.2 55.3 52.5 52.5 50.75 47.25 49 50.75 49.35 49 48.3 49 43.75 47.25 47.6 49 49 49 48.65 43.75 45.85 45.15 45.85 45.15 45.5 46.2 45.5 46.2 45.5 46.2 47.25 46.55 47.6 49 47.25 48.65 48.3 49 49 49 49.35 50.75 52.15 50.75 49 49 49
+300 V	52.15 52.5 52.85 52.85 55.3 56 56.35 57.75 59.15 59.5 55.65 59.5 43.75 48.65 58.8 52.85 55.65 51.8 52.5 52.85 51.8 52.5 50.75 49.35 49 49.35 49 49 47.25 46.9 46.9 48.3 49 49 49 44.8 49 47.95 45.15 47.25 49 46.9 46.9 47.6 49 49 48.65 49 50.75 50.05 50.4 49 51.1 52.15 52.5 52.85 53.9 55.65 54.25 52.15 52.5 52.5 48.65 52.15 51.8 49.7 49 48.3 48.65 45.85 49 44.1 46.55 42.35 45.85 45.5 45.85 47.95 48.65 49 50.75 51.8 52.5 52.85 51.8 52.5 52.5 49 50.75 49 46.2 47.6 47.25 43.75 44.45 45.5 44.8 45.85 45.15 45.5 46.2 47.95 49 47.6 45.85 47.6 48.65 48.3 43.75 47.25 49 49 50.75 45.15 45.5 47.6 49 49.35 47.25 49.35 47.6 48.3 49 49.35 51.1 49 49 49 47.25 46.55 46.9 47.6 49 47.6 47.25 48.65 51.8 47.6 49 49 50.75 52.15 52.5 52.85 53.9 55.3 56 56.35 58.1 59.15

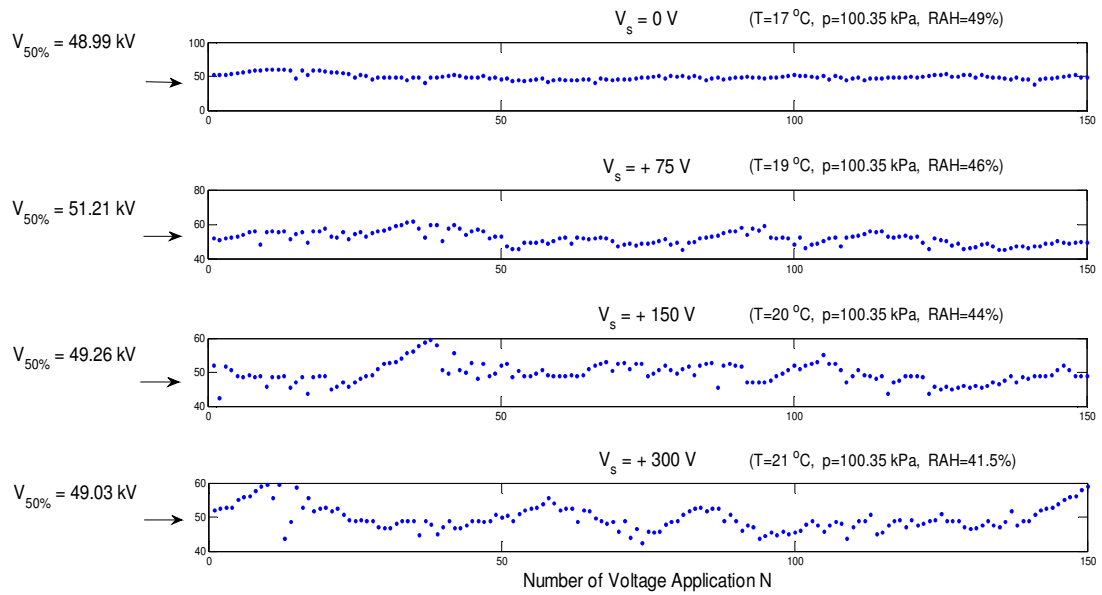


Figure 4. 1 Up-and-down test data for positive sweep voltages. 50% impulse breakdown voltages are indicated.

Table 4.2 shows the normalized up-and-down test data for negative sweep voltages 0 V, -75 V, -150 V, and -300 V. The plots of breakdown test results given in Table 4.2 are shown in Figure 4.2. Assuming the underlying probability distribution for all up-and-down test data is the logistic type distribution, the 50% impulse breakdown voltage values determined by MLE method are also given in Figures 4.2.

Table 4. 2 Negative sweep voltages and STP normalized impulse up-and-down test results

Sweep voltage (V)	Up-and-down test data (kV)
0 V	52.15 48.65 49 48.3 49.35 48.65 47.6 48.65 49 51.45 47.25 45.85 47.25 46.9 45.5 46.2 47.6 46.2 47.6 48.65 49 48.65 49 47.25 49 50.75 42.7 49 47.25 47.6 48.65 48.65 47.6 48.65 49 50.05 49 49.7 52.15 49.7 47.25 47.6 49 49.35 49 47.25 48.65 49.7 47.6 47.95 48.65 48.3 49 49 49 45.5 50.75 47.6 46.55 45.5 46.55 43.75 47.25 48.65 46.9 47.95 47.25 45.5 46.55 45.5 47.25 47.95 49 47.6 49 50.05 49 49.7 48.65 45.85 48.65 48.3 49 49 40.6 49.35 50.4 49.7 49 49 51.45 48.3 51.45 52.5 51.45 47.25 44.8 47.6 46.9 47.6 45.85 45.5 47.25 48.3 48.65 48.3 48.3 47.6 41.65 45.85 45.5 45.85 45.5 45.5 47.25 45.85 47.25 45.5 45.5 45.5 46.9 46.2 47.25 48.3 47.95 43.75 45.15 45.5 45.5 44.1 45.15 45.5 47.6 45.85 46.9 47.25 47.25 45.85 45.15 45.5 46.9 44.8 46.9 47.25 46.9 47.6 49 47.95 48.65 50.4
-75 V	50.4 45.85 51.1 49.35 48.65 49.35 50.4 51.45 52.5 51.45 52.15 49.35 48.65 49 47.6 44.45 44.45 42.35 44.8 45.5 45.85 45.5 46.55 47.6 48.65 49.35 49.7 46.55 47.6 47.6 46.2 45.85 45.85 45.5 44.1 45.15 44.8 45.85 46.2 47.6 48.3 49 47.6 43.75 46.55 44.8 46.725 45.85 46.55 47.6 47.6 47.6 48.3 45.675 48.3 49.35 50.4 47.95 44.8 45.85 45.85 45.15 44.8 45.85 46.9 44.8 45.5 45.15 44.8 45.85 46.55 47.6 48.65 49 49 48.65 42 47.6 48.3 46.2 48.3 49 50.05 47.6 50.05 51.1 50.05 51.1 52.15 51.1 50.05 47.775 47.6 44.8 46.55 47.6 48.65 44.8 46.55 47.6 48.3 49.7 47.6 47.6 46.9 47.25 46.9 47.6 48.65 46.2 45.15 45.85 46.55 47.6 44.1 46.2 46.55 47.6 46.9 45.85 46.9 47.6 48.3 49 50.4 50.05 50.4 49.35 48.3 46.55 48.3 47.6 47.95 49 50.05 51.1 47.95 49 50.4 49.7 50.05 51.1 50.4 47.25 48.3 49 44.8 47.25 47.075 47.25
-150 V	52.15 52.5 47.6 52.5 49.35 49 52.15 50.05 48.3 47.95 47.25 47.95 49 49 46.55 47.95 47.25 46.55 44.1 44.45 43.75 42.35 43.75 42 43.4 42.7 42.7 44.1 43.75 43.75 45.15 45.5 47.25 42 45.15 45.5 47.25 47.6 42.35 48.3 48.3 47.25 46.9 47.6 49 49.35 50.75 50.4 47.6 49 49 49 50.75 48.3 50.4 49 48.65 49.35 49.7 49 45.85 47.6 48.65 49 45.5 49 45.5 47.6 44.625 45.5 44.8 45.15 45.15 45.5 47.25 45.5 45.15 45.5 44.8 45.5 46.2 47.95 48.65 49 50.4 49 50.75 48.65 48.65 49 50.4 52.15 52.5 47.25 52.5 47.6 50.4 49 45.5 47.25 46.9 47.6 48.65 49 45.15 47.6 44.8 47.95 47.6 47.6 49 45.5 48.65 49 50.75 45.5 50.75 48.65 47.95 45.5 46.2 45.5 46.2 47.6 48.65 47.25 48.65 47.25 43.75 47.6 45.15 45.5 46.55 45.5 46.9 45.15 45.5 44.275 44.8 44.1 43.05 43.4 45.15 45.5 45.85 47.6 45.5 46.9 46.2 47.6
-300 V	50.75 52.5 53.2 53.55 54.95 55.65 56 57.4 56.35 56 50.75 56 54.6 52.5 52.5 49.7 48.65 47.25 49 49.35 47.6 43.75 46.55 46.55 46.55 45.85 47.25 45.5 47.95 45.5 45.15 45.5 47.25 42.7 44.8 44.45 43.05 44.45 45.15 45.5 46.55 47.6 48.65 49.35 48.3 46.2 46.2 47.6 45.85 47.95 49 47.6 46.2 47.25 43.75 47.25 48.65 49 49 50.05 45.5 52.15 48.65 47.25 47.95 49 47.95 48.65 49 48.65 49.35 38.5 45.5 43.75 45.15 44.8 45.5 46.55 47.25 48.3 47.25 48.65 49.35 50.75 52.15 52.5 52.85 52.5 49 52.5 52.5 52.85 54.25 52.5 54.95 43.75 49.35 50.75 48.65 52.5 52.15 45.85 51.8 52.5 51.45 49.35 52.15 50.75 49.35 48.65 47.6 48.3 47.6 46.2 45.5 46.55 45.5 36.75 40.6 42.35 42 42.35 43.75 45.15 42 44.45 45.5 45.85 47.6 48.3 49 48.65 49 50.4 49.7 44.8 49 45.85 48.65 50.05 51.1 51.45 43.4 49.7 44.8 48.3 49 50.05 51.1

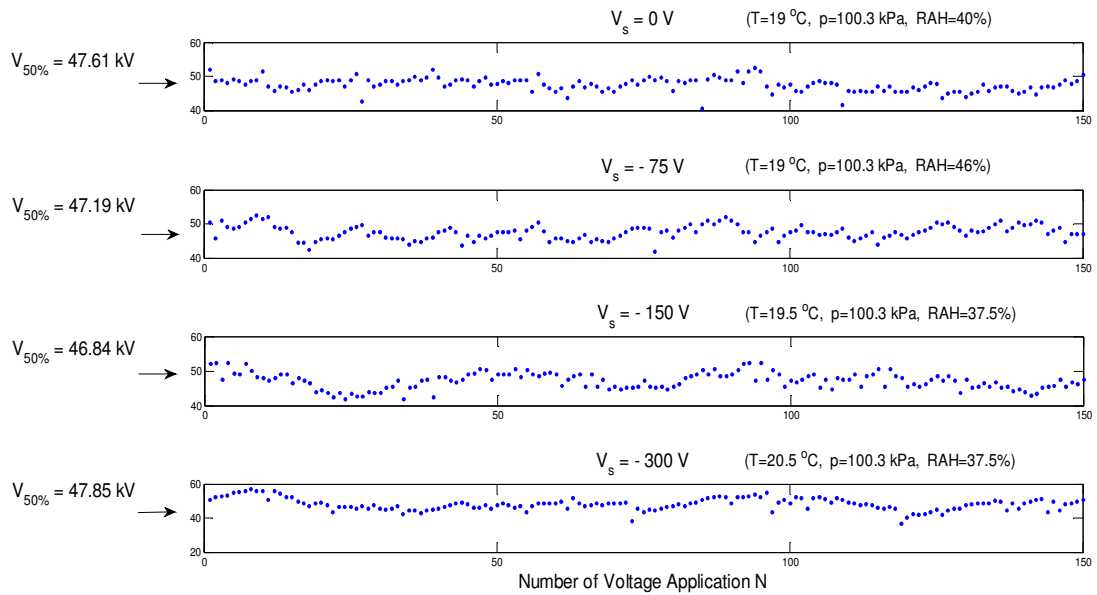


Figure 4. 2 Up-and-down test data for negative sweep voltages. 50% impulse breakdown voltages are indicated.

4.2 Results of Parameter Estimates

As explained in Section 2.3, four distribution functions are generally applied to represent distribution of the impulse breakdown voltage for self-restoring insulation systems: Normal, logistic 3PW, and Gumbel distributions. The parameters of these distributions are estimated from the up-and-down test data. Also, in Section 2.4, utilization of the MLE method for evaluation of the parameters of these distributions were explained. The reason for selecting the MLE method is because of its its well known accurate outcomes in statistical assesments. For optimization of the MLE equations (Appendix A.1) the Monte Carlo (MC) and the Newton-Raphon (N-R) methods are employed to ensure the accurate estimates with less number of iterations. The results of parameter estimates for positive and negative sweep voltages data are shown in Tables 4.3 and 4.4.

As is observed in Table 4.3, the parameter estimates of four distributions obtained with the MC and N-R methods are close to each other for all positive sweep voltages except the sweep voltage + 75 V. The parameter estimates of four distributions for this sweep voltage are appreciably different from the other estimates obtained for the other sweep fields.

Somerville and Tedford have shown that statistical time-lag and impulse breakdown strength of SF₆ in a gas vessel are affected by sweep voltages [10,11]. However, in the present study the MLEs of the positive impulse breakdown voltage data are not influenced much by the sweep fields. This may be due to the fact that during the present experiments no artificial radiation source was used.

Table 4. 3 Maximum likelihood estimates for positive sweep voltage data.

Sweep Voltage	Dist. Type	MC Opt	N-R Opt
0 V	ND	$\hat{\theta}_1=(49.1949, 4.3738)$	$\hat{\theta}_1=(49.1959, 4.3685)$
	LD	$\hat{\theta}_2=(48.9953, 2.3993)$	$\hat{\theta}_2=(48.9952, 2.3986)$
	3PWD	$\hat{\theta}_3=(14.0028, 3.0510, 36.7128)$	$\hat{\theta}_3=(13.8305, 3.0086, 36.8138)$
	GD	$\hat{\theta}_4=(4.7628, 51.4372)$	$\hat{\theta}_4=(4.7614, 51.4373)$
+ 75 V	ND	$\hat{\theta}_1=(51.3760, 3.7909)$	$\hat{\theta}_1=(51.3757, 3.7891)$
	LD	$\hat{\theta}_2=(51.2159, 2.2155)$	$\hat{\theta}_2=(51.2156, 2.2160)$
	3PWD	$\hat{\theta}_3=(7.8761, 1.9218, 44.4437)$	$\hat{\theta}_3=(7.6477, 1.8408, 44.6049)$
	GD	$\hat{\theta}_4=(3.9077, 53.2685)$	$\hat{\theta}_4=(3.9055, 53.2834)$
+ 150 V	ND	$\hat{\theta}_1=(49.2607, 2.8397)$	$\hat{\theta}_1=(49.2561, 2.8474)$
	LD	$\hat{\theta}_2=(49.2636, 1.5728)$	$\hat{\theta}_2=(49.2674, 1.5727)$
	3PWD	$\hat{\theta}_3=(9.3833, 3.2282, 40.7559)$	$\hat{\theta}_3=(9.5516, 3.2510, 40.6727)$
	GD	$\hat{\theta}_4=(3.1151, 50.6441)$	$\hat{\theta}_4=(3.1115, 50.6539)$
+ 300 V	ND	$\hat{\theta}_2=(49.1023, 3.2930)$	$\hat{\theta}_2=(49.1052, 3.2984)$
	LD	$\hat{\theta}_2=(49.0370, 1.8892)$	$\hat{\theta}_2=(49.0322, 1.8910)$
	3PWD	$\hat{\theta}_3=(8.8184, 2.5912, 41.1790)$	$\hat{\theta}_3=(8.7913, 2.5343, 41.3095)$
	GD	$\hat{\theta}_4=(3.5515, 50.7447)$	$\hat{\theta}_4=(3.5545, 50.7460)$

ND: Normal Distribution, $\hat{\theta}_1 = (\hat{\mu}, \hat{\sigma})$ (in kV);

LD: Logistic Distribution, $\hat{\theta}_2 = (\hat{\mu}, \hat{s})$ (in kV);

3PWD: Three-parameter Weibull Distribution, $\hat{\theta}_3 = (\hat{\alpha}, \hat{\beta}, \hat{\gamma})$ (in kV);

GD: Gumbel Distribution, $\hat{\theta}_4 = (\hat{\alpha}, \hat{\beta})$ (in kV).

The parameter estimates of four distributions obtained with the MC and N-R methods for the all negative sweep voltages are given in Table 4.4. The parameter estimates are remarkably close to each other.

Table 4. 4 Maximum likelihood estimates for negative sweep voltage data.

Sweep Voltage	Dist. Type	MC Opt	N-R Opt
0 V	ND	$\hat{\theta}_1=(47.5616, 2.4315)$	$\hat{\theta}_1=(47.5565, 2.4288)$
	LD	$\hat{\theta}_2=(47.6041, 1.3791)$	$\hat{\theta}_2=(47.6108, 1.3792)$
	3PWD	$\hat{\theta}_3=(12.0656, 5.1940, 36.4312)$	$\hat{\theta}_3=(12.3427, 5.3660, 36.1514)$
	GD	$\hat{\theta}_4=(2.2504, 48.6952)$	$\hat{\theta}_4=(2.2489, 48.6958)$
- 75 V	ND	$\hat{\theta}_1=(47.2615, 2.3956)$	$\hat{\theta}_1=(47.2639, 2.3989)$
	LD	$\hat{\theta}_2=(47.2016, 1.4149)$	$\hat{\theta}_2=(47.1949, 1.4198)$
	3PWD	$\hat{\theta}_3=(7.2208, 2.9168, 40.8867)$	$\hat{\theta}_3=(7.2310, 2.9448, 40.8223)$
	GD	$\hat{\theta}_4=(2.3343, 48.4341)$	$\hat{\theta}_4=(2.3406, 48.4308)$
- 150 V	ND	$\hat{\theta}_1=(46.8637, 2.2760)$	$\hat{\theta}_1=(46.8743, 2.2706)$
	LD	$\hat{\theta}_2=(46.8474, 1.3253)$	$\hat{\theta}_2=(46.8435, 1.3273)$
	3PWD	$\hat{\theta}_3=(6.8974, 2.9175, 40.7225)$	$\hat{\theta}_3=(6.7806, 2.9089, 40.8367)$
	GD	$\hat{\theta}_4=(2.2936, 47.9866)$	$\hat{\theta}_4=(2.2979, 47.9829)$
- 300 V	ND	$\hat{\theta}_1=(47.8055, 3.7486)$	$\hat{\theta}_1=(47.8077, 3.7555)$
	LD	$\hat{\theta}_2=(47.8476, 2.0669)$	$\hat{\theta}_2=(47.8507, 2.0680)$
	3PWD	$\hat{\theta}_3=(17.3321, 4.6303, 31.8752)$	$\hat{\theta}_3=(17.3131, 4.6931, 31.9167)$
	GD	$\hat{\theta}_4=(3.6964, 49.6185)$	$\hat{\theta}_4=(3.7015, 49.6169)$

ND: Normal Distribution, $\hat{\theta}_1 = (\hat{\mu}, \hat{\sigma})$ (in kV);

LD: Logistic Distribution, $\hat{\theta}_2 = (\hat{\mu}, \hat{s})$ (in kV);

3PWD: Three-parameter Weibull Distribution, $\hat{\theta}_3 = (\hat{\alpha}, \hat{\beta}, \hat{\gamma})$ (in kV);

GD: Gumbel Distribution, $\hat{\theta}_4 = (\hat{\alpha}, \hat{\beta})$ (in kV).

4.3 Discussion of Kolmogorov-Smirnov Test Results

To determine the most fitting distribution function, among the normal, logistic and Gumbel distributions, to the up-and-down tests data for various sweep voltages, the K-S tests are applied [20-22]. The results are shown in Tables 4.5 and 4.6.

The Gumbel distribution seems to be the most unfitting distribution for all impulse breakdown data under all sweep voltages because of its large K-S outcomes (Table 4.5 and 4.6)

Also, the small K-S values determined for the logistic distribution indicates that it serves better than both the normal and Gumbel distributions for the set of all positive sweep voltage data as illustrated in Table 4.5.

Table 4. 5 Kolmogorov Smirnov test results for positive sweep voltage data.

Sweep Voltage	Dist. Type	MLE	K-S
0 V	ND	$\hat{\theta}_1 = (49.1959, 4.3685)$	0.1896
	LD	$\hat{\theta}_2 = (48.9952, 2.3986)$	0.1807
	GD	$\hat{\theta}_3 = (4.7614, 51.4373)$	0.2079
+ 75 V	ND	$\hat{\theta}_1 = (51.3757, 3.7891)$	0.1524
	LD	$\hat{\theta}_2 = (51.2156, 2.2160)$	0.1329
	GD	$\hat{\theta}_3 = (3.9055, 53.2834)$	0.2010
+ 150 V	ND	$\hat{\theta}_1 = (49.2561, 2.8474)$	0.1279
	LD	$\hat{\theta}_2 = (49.2674, 1.5727)$	0.1263
	GD	$\hat{\theta}_3 = (3.1115, 50.6539)$	0.1617
+ 300 V	ND	$\hat{\theta}_1 = (49.1052, 3.2984)$	0.1033
	LD	$\hat{\theta}_2 = (49.0322, 1.8910)$	0.0999
	GD	$\hat{\theta}_3 = (3.5545, 50.7460)$	0.1506

ND: Normal Distribution, $\hat{\theta}_1 = (\hat{\mu}, \hat{\sigma})$ (in kV);

LD: Logistic Distribution, $\hat{\theta}_2 = (\hat{\mu}, \hat{s})$ (in kV);

GD: Gumbel Distribution, $\hat{\theta}_3 = (\hat{\alpha}, \hat{\beta})$ (in kV).

As is indicated in Table 4.6, in the case of all negative sweep voltages impulse breakdown voltage data the logistic distribution performs better than other distributions for the only set of sweep voltages -75 V and -300 V. On the other hand, the normal distribution outperforms the logistic and Gumbel distributions for the sweep voltages 0 V and -150 V similar to the results obtained in references [20-22].

Table 4. 6 Kolmogorov Smirnov test results for negative sweep voltage data.

Sweep Voltage	Dist. Type	MLE	K-S
0 V	ND	$\hat{\theta}_1=(47.5565, 2.4288)$	0.1199
	LD	$\hat{\theta}_2=(47.6108, 1.3792)$	0.1362
	GD	$\hat{\theta}_3=(2.2489, 48.6958)$	0.1580
- 75 V	ND	$\hat{\theta}_1=(47.2639, 2.3989)$	0.1182
	LD	$\hat{\theta}_2=(47.1949, 1.4198)$	0.1032
	GD	$\hat{\theta}_3=(2.3406, 48.4308)$	0.1696
- 150 V	ND	$\hat{\theta}_1=(46.8743, 2.2706)$	0.1223
	LD	$\hat{\theta}_2=(46.8435, 1.3273)$	0.1279
	GD	$\hat{\theta}_3=(2.2979, 47.9829)$	0.1397
- 300 V	ND	$\hat{\theta}_1=(47.8077, 3.7555)$	0.1299
	LD	$\hat{\theta}_2=(47.8507, 2.0680)$	0.1169
	GD	$\hat{\theta}_3=(3.7015, 49.6169)$	0.1833

ND: Normal Distribution, $\hat{\theta}_1 = (\hat{\mu}, \hat{\sigma})$ (in kV);

LD: Logistic Distribution, $\hat{\theta}_2 = (\hat{\mu}, \hat{s})$ (in kV);

GD: Gumbel Distribution, $\hat{\theta}_3 = (\hat{\alpha}, \hat{\beta})$ (in kV).

4.4 Discussion of Likelihood Ratio Test Results

Because of distinctive feature of the logistic distribution in representing the impulse breakdown test data and its outstanding performance better than the other two-

parameter distributions, as a next step, its performance is compared it with three-parameter Weibull distribution. As explained in Section 2.5.2, for this purpose the likelihood ratio (LR) test is applied [15] at 5% significance level which allows to figure out whether the test data comes from the logistic or the 3PW distributions.

Table 4. 7 Likelihood ratio test results for positive sweep voltage data.

Sweep Voltage	Dist. Type	MLE	LL value	R	p-value
0 V	LD	$\hat{\theta}_1=(48.9952, 2.3986)$	-216.3519	4.0218	0.0449
	3PWD	$\hat{\theta}_2=(13.8305, 3.0086, 36.8138)$	-218.3628		
+ 75 V	LD	$\hat{\theta}_1=(51.2156, 2.2160)$	-206.4928	10.1708	0.0014
	3PWD	$\hat{\theta}_2=(7.6477, 1.8408, 44.6049)$	-201.4074		
+ 150 V	LD	$\hat{\theta}_1=(49.2674, 1.5727)$	-181.4788	3.7128	0.0540
	3PWD	$\hat{\theta}_2=(9.5516, 3.2510, 40.6727)$	-183.3352		
+ 300 V	LD	$\hat{\theta}_1=(49.0322, 1.8910)$	-178.3459	2.4346	0.1187
	3PWD	$\hat{\theta}_2=(8.7913, 2.5343, 41.3095)$	-177.1286		

LD: Logistic Distribution, $\hat{\theta}_1 = (\hat{\mu}, \hat{s})$ (in kV);

3PWD: Three-parameter Weibull Distribution, $\hat{\theta}_2 = (\hat{\alpha}, \hat{\beta}, \hat{\gamma})$ (in kV).

R: Likelihood ratio test statistic value;

LL: Log-likelihood value.

Since the LR test provides information to compare the goodness-of-fit of two distributions namely logistic and 3PW distributions, following the steps of the test, which requires determining χ^2 distribution from the LR test statistics (R) (Equation 2.31), then resulting p -value (Equation 2.34) allows to determine the type of statistical distribution.

The LR test statistics requires χ^2 limit to be 3.841 at $k=1$ degrees of freedom and the corresponding p -value to be 0.05 at 5% significance level. Under this requisite R values smaller than 3.841 and p -values greater than 0.005, denote that logistic distribution fits better than 3PW distribution to the test data. As shown in Tables 4.7 and 4.8, for sweep voltages 0 V, -300 V and +150 V, +300 V, the impulse

breakdown data samples, logistic distribution serves better than 3PW distribution since all R values remain less than 3.842 limit and p -values become greater than 0.005.

On the other hand, for sweep voltages 0 V, +75 V, -75 V and -150 V, the impulse breakdown data samples fit well to 3PW distribution rather than logistic distribution according to LR test (Tables 4.7 and 4.8), since R and $1-p$ values remain less than the prerequisites.

Table 4. 8 Likelihood ratio test results for negative sweep voltage data.

Sweep Voltage	Dist. Type	MLE	LL value	R	P-value
0 V	LD	$\hat{\theta}_1=(47.6108, 1.3792)$	-170.4623	0.0388	0.8438
	3PWD	$\hat{\theta}_2=(12.3427, 5.3660, 36.1514)$	-170.4817		
- 75 V	LD	$\hat{\theta}_1=(47.1949, 1.4198)$	-172.5591	4.5044	0.0338
	3PWD	$\hat{\theta}_2=(7.231036, 2.9448, 40.8223)$	-170.3069		
- 150 V	LD	$\hat{\theta}_1=(46.8435, 1.3273)$	-169.5264	3.9018	0.0482
	3PWD	$\hat{\theta}_2=(6.7806, 2.9089, 40.8367)$	-167.5755		
- 300 V	LD	$\hat{\theta}_1=(47.8507, 2.0680)$	-191.6012	3.6278	0.0568
	3PWD	$\hat{\theta}_2=(17.3131, 4.6931, 31.9167)$	-193.4151		

LD: Logistic Distribution, $\hat{\theta}_1 = (\hat{\mu}, \hat{\delta})$ (in kV);

3PWD: Three-parameter Weibull Distribution, $\hat{\theta}_2 = (\hat{\alpha}, \hat{\beta}, \hat{\gamma})$ (in kV).

R: Likelihood ratio test statistic value;

LL: Log-likelihood value.

4.5 Discussion of Quantile-Quantile Plots

A visual comparative study for deciding the best fitted distribution to the impulse breakdown data, which is performed under positive and negative DC sweep voltages, is carried out with Quantile-Quantile (Q-Q) plots. Since $F^{-1}(p_i)$ provides the impulse breakdown voltage estimates, the closest value of $F^{-1}(p_i)$ to the actual impulse breakdown voltage allows us to determine the most fitted distribution

function. In these plots the percentile p_i is taken to be $(i-0.5)/n$ [20]. Figures 4.3, 4.4, 4.5 and 4.6 show the Q-Q plots of normal, logistic, Gumbel and three-parameter Weibull distributions for sweep voltages 0 V (Figure 4.3), +75 V (Figure 4.4), +150 V (Figure 4.5), and +300 V (Figure 4.6), respectively. The results of these plots confirm the results of LR and K-S tests. That is, the logistic distribution fits well to the test data for +150 V and +300 V sweep voltages. Gumbel is the most incompatible among four distributions. Normal, logistic and 3PW distributions seem to be acceptable for all positive sweep voltage data.

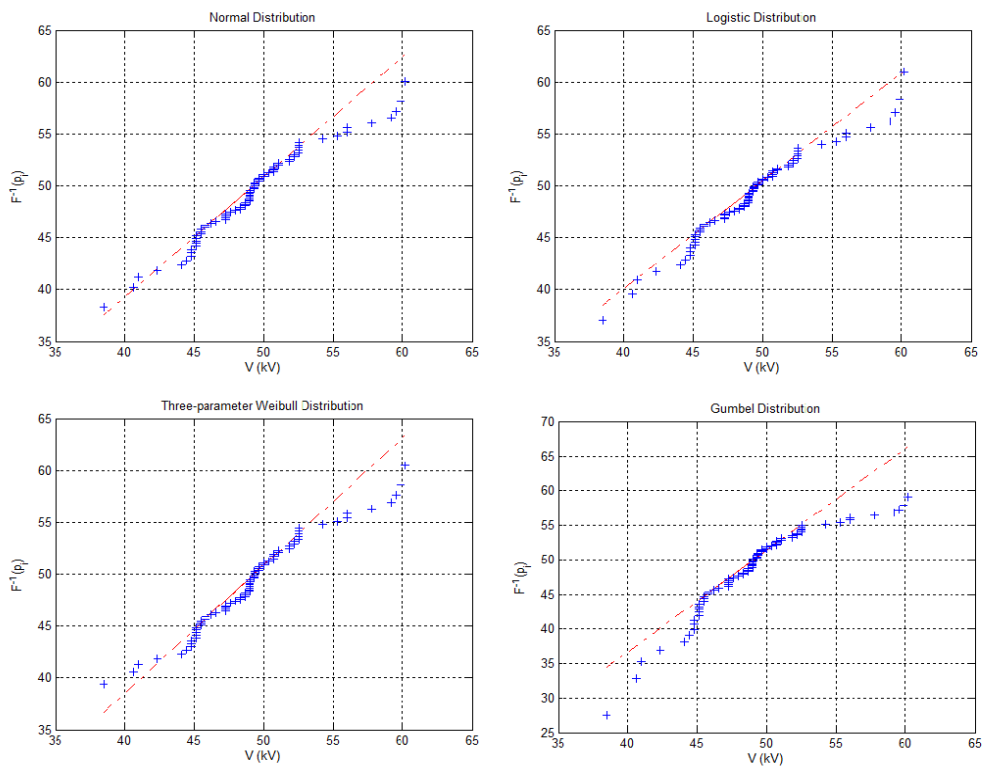


Figure 4. 3 Q-Q plots of four distributions for 0 V sweep voltage data.

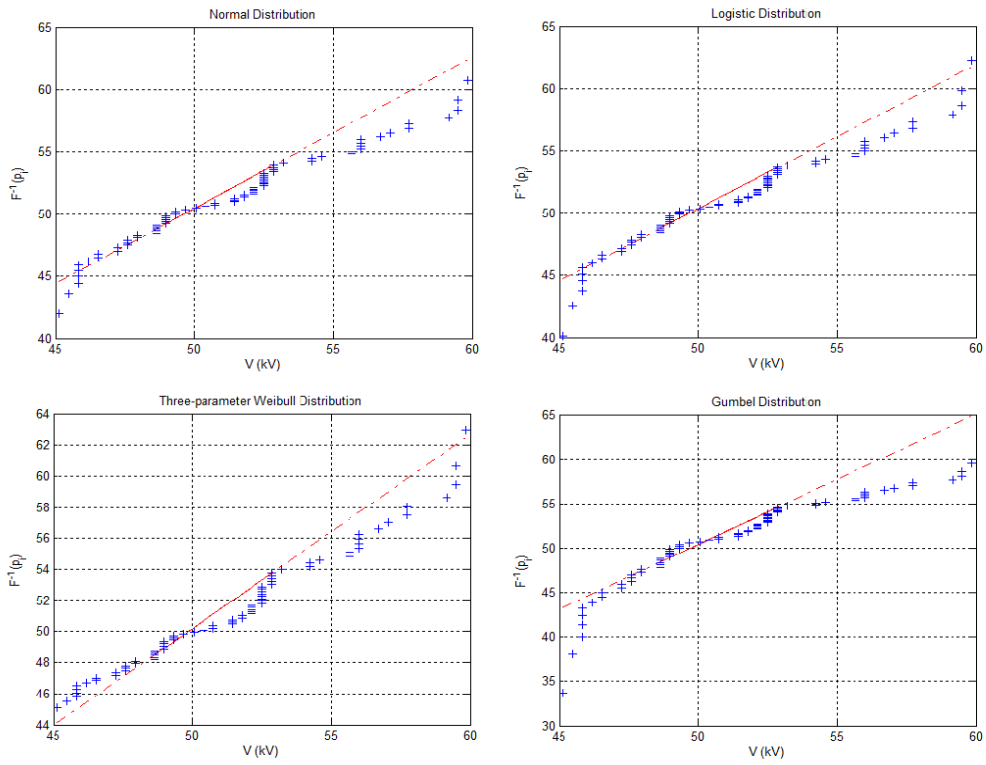


Figure 4. 4 Q-Q plots of four distributions for + 75 V sweep voltage data.

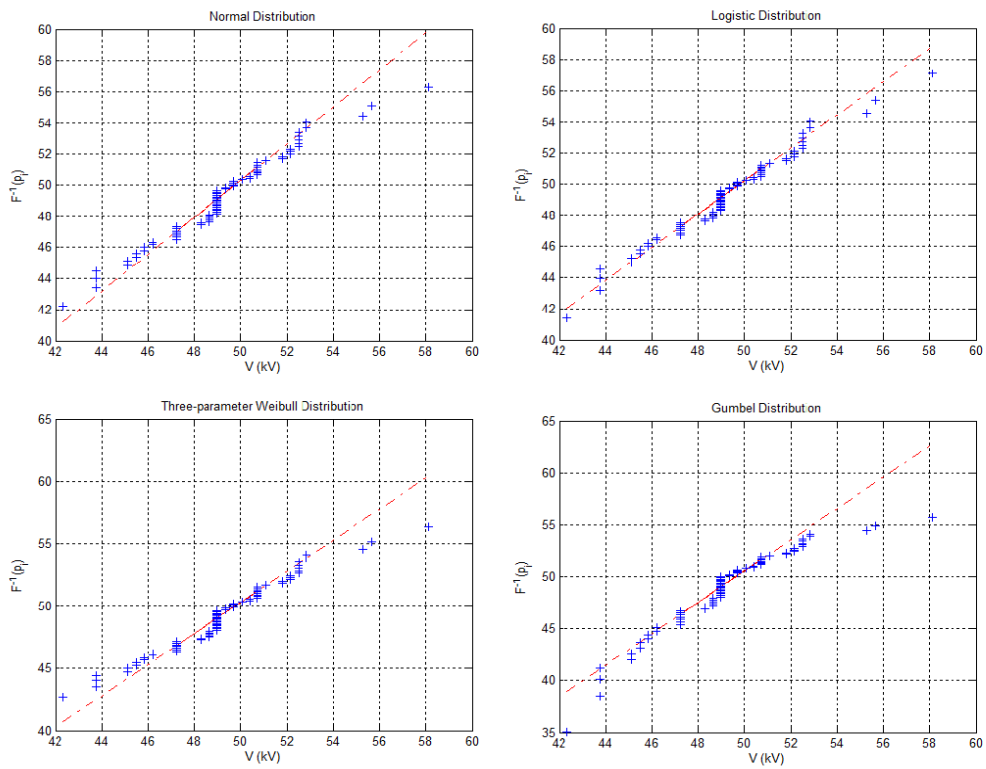


Figure 4. 5 Q-Q plots of four distributions for + 150 V sweep voltage data.

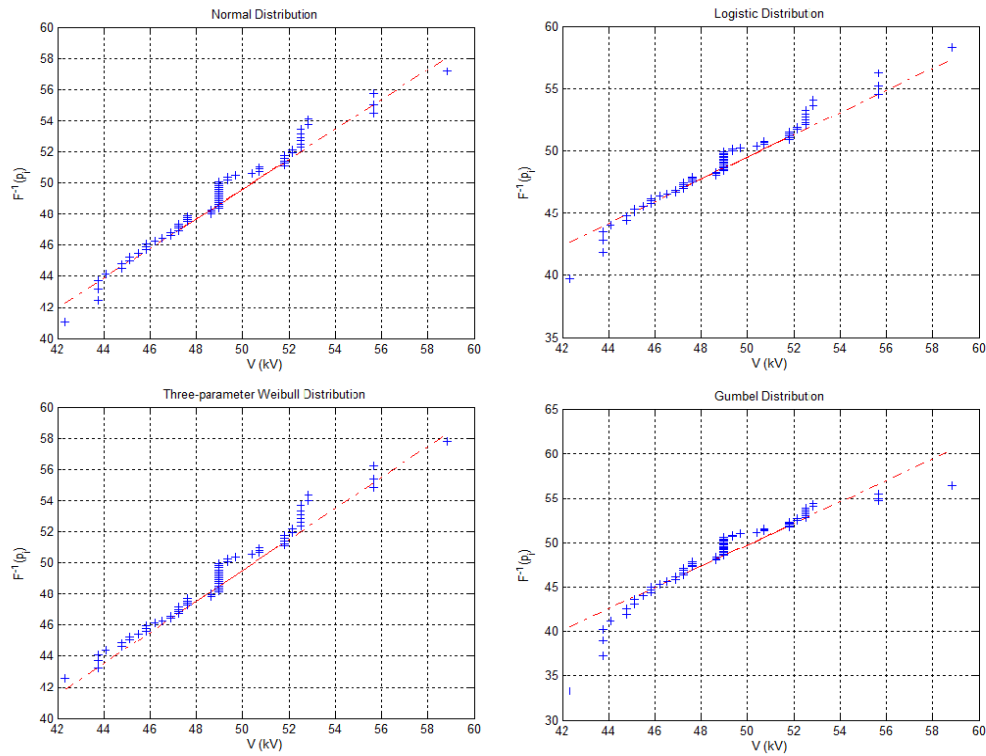


Figure 4. 6 Q-Q plots of four distributions for + 300 V sweep voltage data.

Figures 4.7, 4.8, 4.9, and 4.10 show the Q-Q plots of normal, logistic, Gumbel and 3PW distributions for sweep voltages 0 V (Figure 4.7), -75 V (Figure 4.8), -150 V (Figure 4.9), and -300 V (Figure 4.10), respectively. The results of these plots confirm the results of LR and K-S tests. That is, the logistic distribution fits well to the test data for 0V and -300 V sweep voltages. The Gumbel distribution is also the most improper among four distributions for all negative sweep voltage data. It may be concluded that normal and 3PW distributions can be used well enough to model negative sweep voltage data.

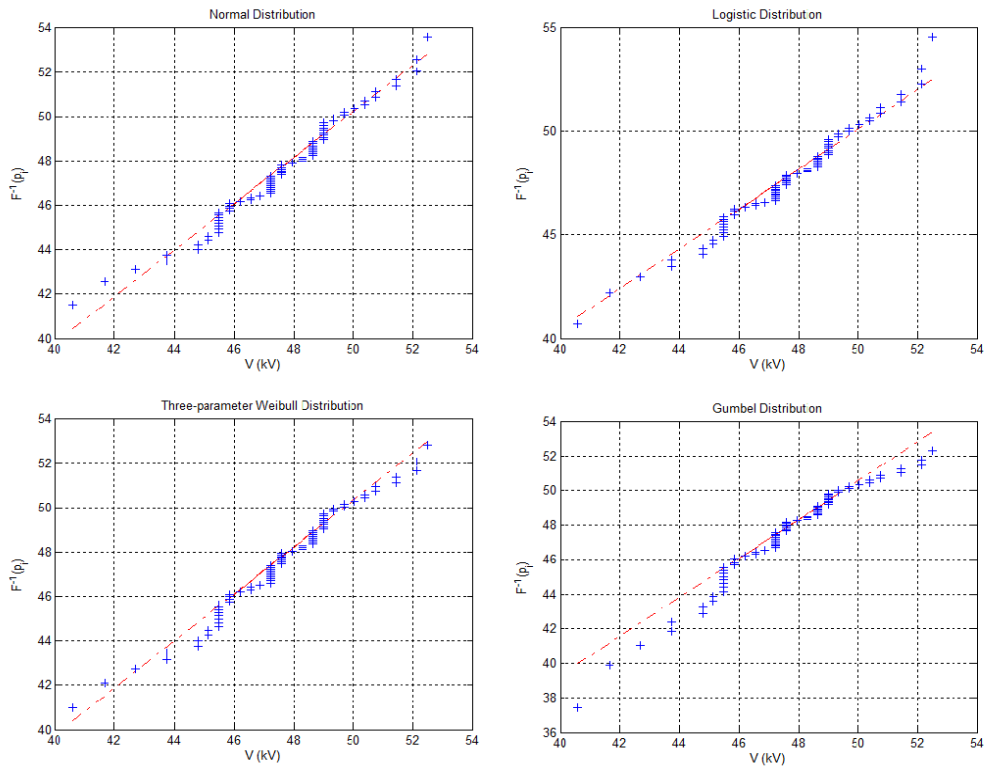


Figure 4.7 Q-Q plots of four distributions for 0 V sweep voltage data.

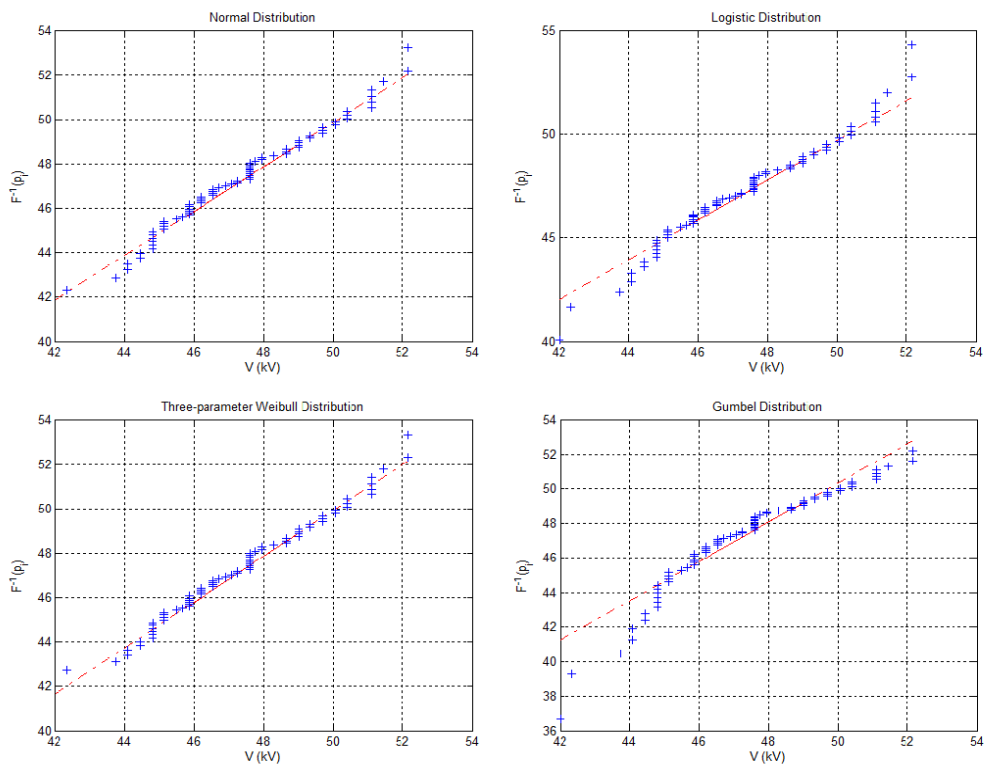


Figure 4.8 Q-Q plots of four distributions for -75 V sweep voltage data.

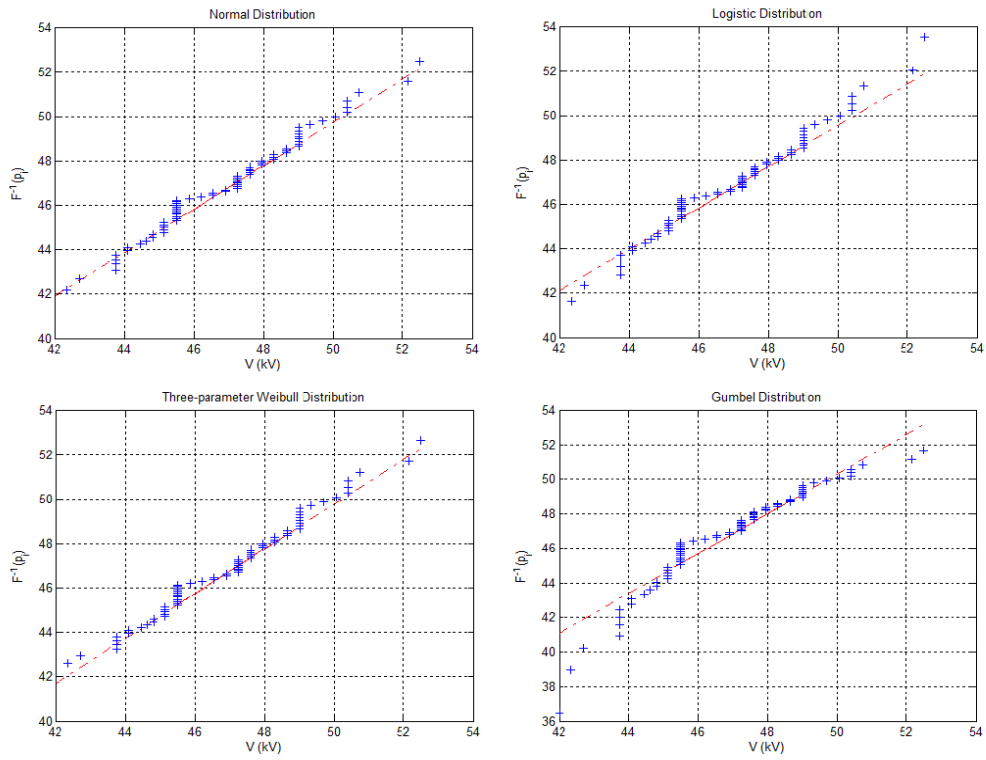


Figure 4.9 Q-Q plots of four distributions for - 150 V sweep voltage data.

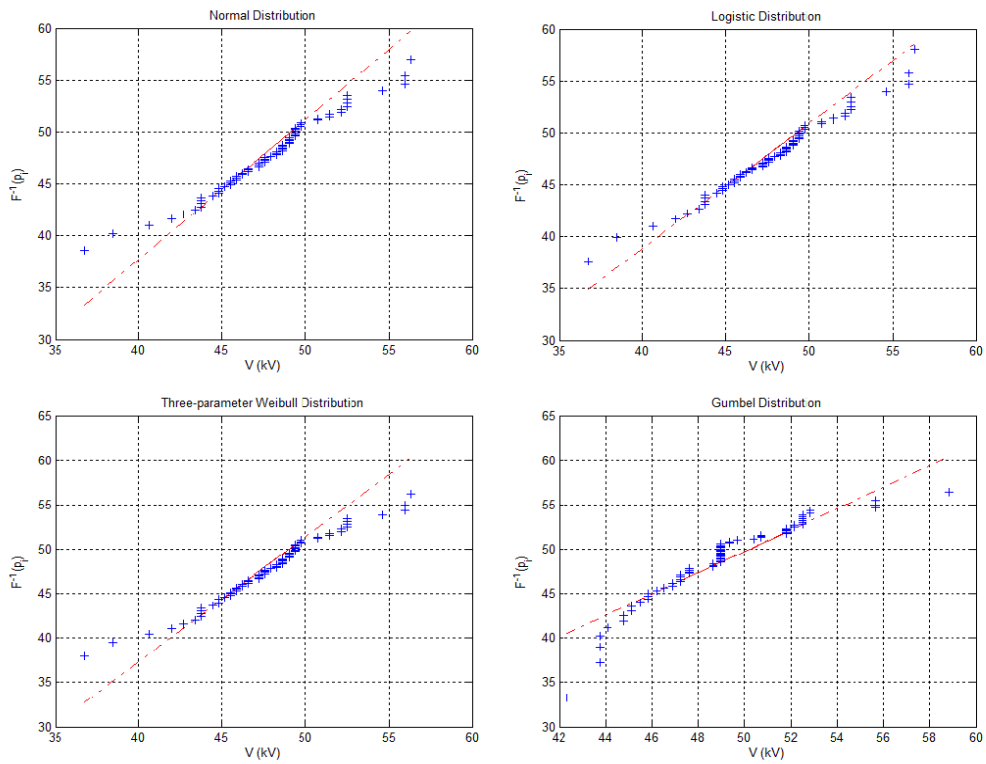


Figure 4.10 Q-Q plots of four distributions for - 300 V sweep voltage data.

4.6 Logistic Plots of Various Sweep Voltages Data and Confidence Limits

For theoretical justification of the logistic distribution as an alternative to commonly used normal, 3PW and Gumbel distributions, whether the distribution of impulse breakdown data for positive sweep voltages lies within 95% confidence interval or not is shown on $\ln(p/(1-p))$ versus impulse breakdown voltage, V plot. In Figures 4.11-4.14 logistic plots for impulse breakdown voltage data for positive sweep voltages and in Figures 4.15-4.18 logistic plots for impulse breakdown voltage data for negative sweep voltages are shown.

For sweep voltages 0 V (Figure 4.11), +150 V (Figure 4.13), and +300 V (Figure 4.14) the data points remain well enough within 95% limits. However, for the sweep voltage +75 V (Figure 4.12) there is a slight skewness such that the data falls out of the limits at lower probability level.

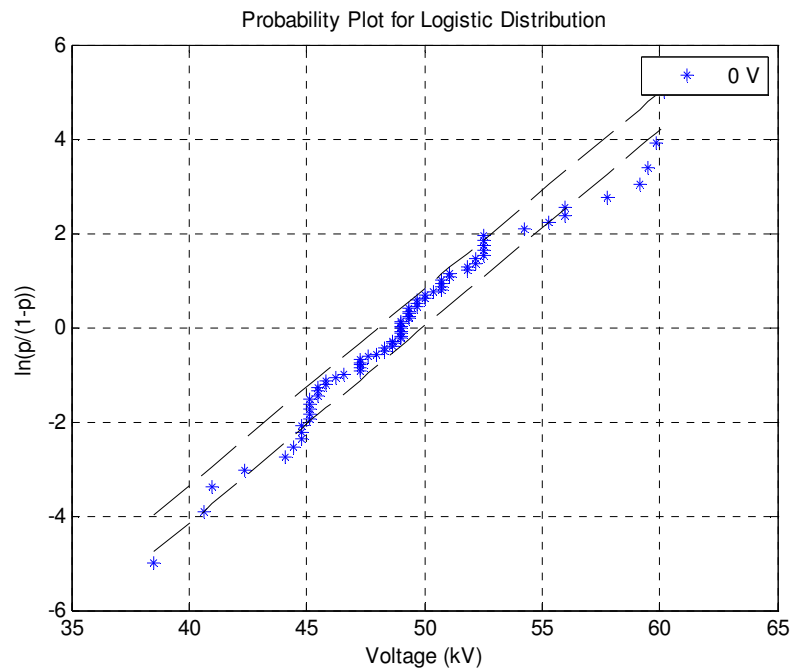


Figure 4.11 Logistic plot of 0 V sweep voltage data and 95% confidence limits.

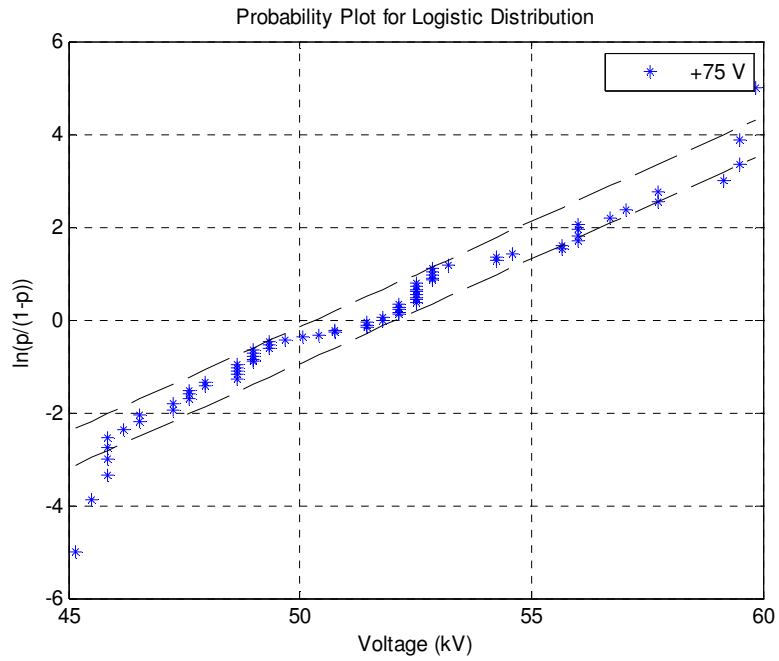


Figure 4.12 Logistic plot of + 75 V sweep voltage data and 95% confidence limits.

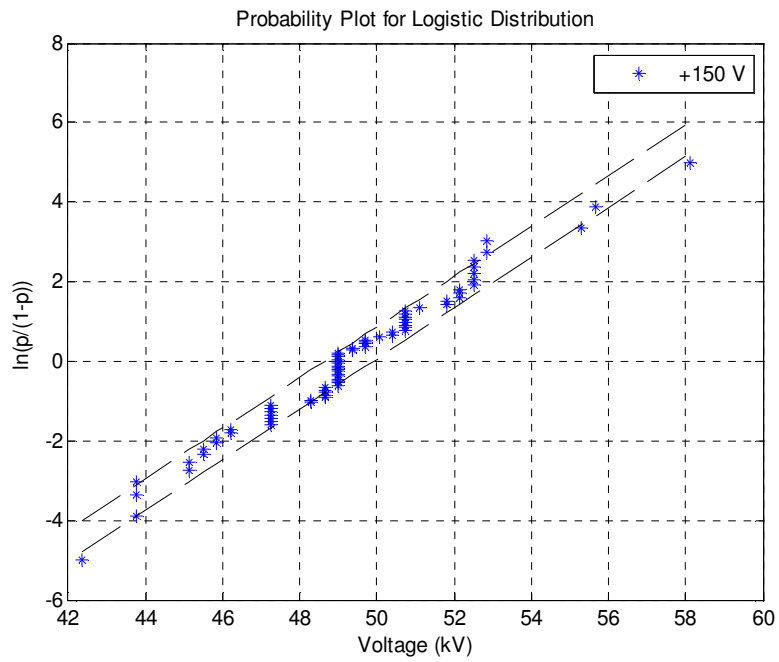


Figure 4.13 Logistic plot of + 150 V sweep voltage data and 95% confidence limits.

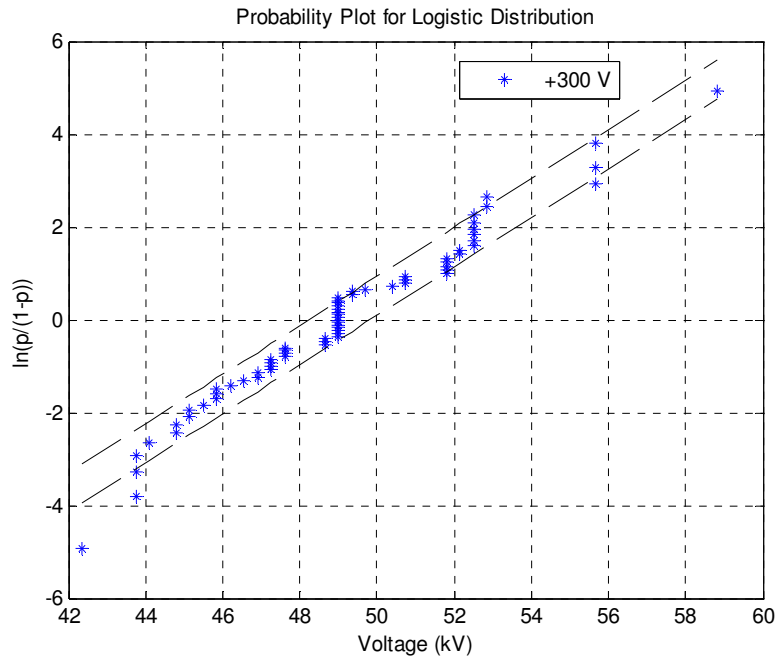


Figure 4.14 Logistic plot of + 300 V sweep voltage data and 95% confidence limits.

Similarly, for sweep voltages 0 V (Figure 4.15), -150 V (Figure 4.17), and -300 V (Figure 4.18) almost all the breakdown data points are observed to lie within 95% limits. Still, there is a slight exclusion of the data for the sweep voltage -75 V (Figure 4.16) out of the 95% tolerance bounds i.e., there is a slight skewness of the data at lower probability level.

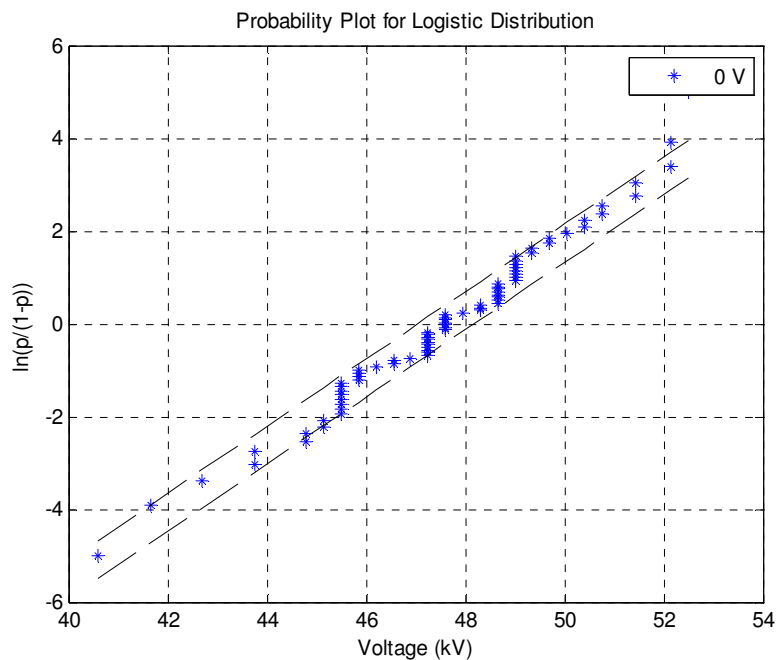


Figure 4.15 Logistic plot of 0 V sweep voltage data and 95% confidence limits.

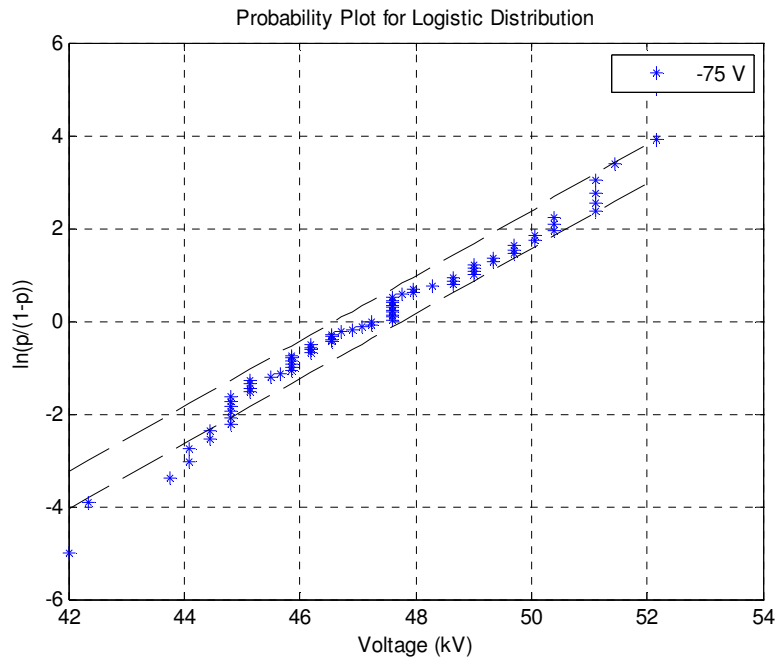


Figure 4.16 Logistic plot of - 75 V sweep voltage data and 95% confidence limits.

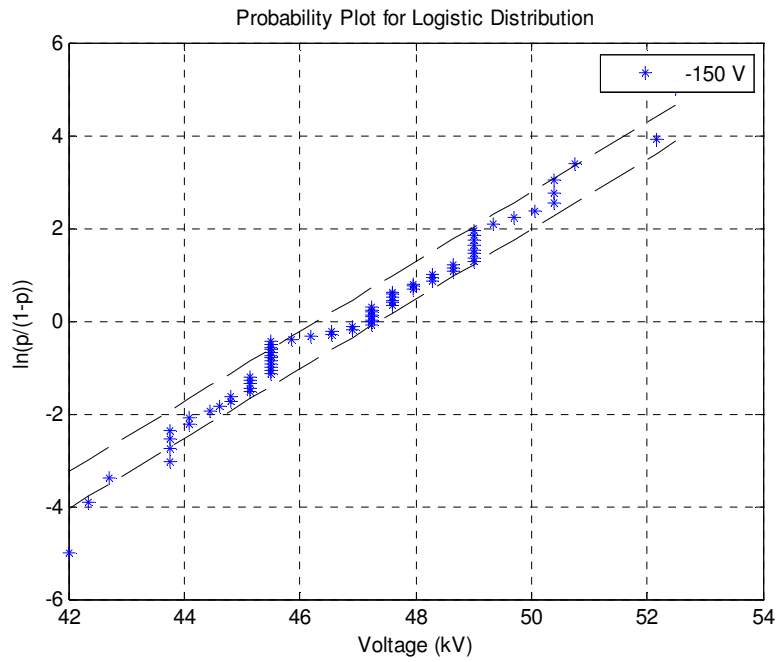


Figure 4.17 Logistic plot of - 150 V sweep voltage data and 95% confidence limits.

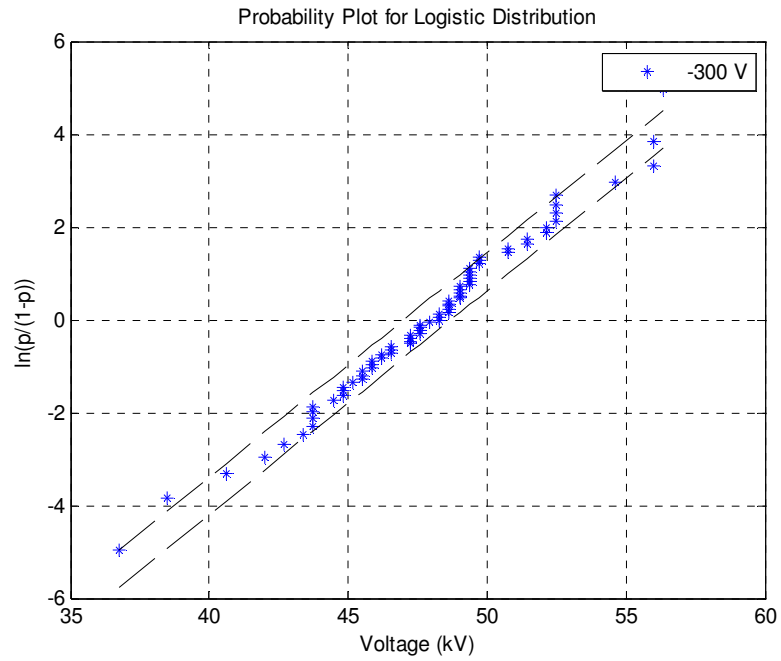


Figure 4.18 Logistic plot of - 300 V sweep voltage data and 95% confidence limits.

Hence, we can conclude that the statistical distribution of the data for positive and negative sweep voltages of the present experimental work is statistically sufficient to be represented by logistic distribution within the acceptable confidence limits.

4.7 Experimental Time-Lag Results

The graphical representation showing a visual distribution of the statistical time-lag data of positive impulse breakdown voltage are observed to be skewed toward zero time-lag as illustrated in the histograms in the plots of Figure 4.19 for positive sweep voltages and in the plots of Figure 4.20 for negative sweep voltages. Hence, the distribution of time lags is likely to be exponential type [10]. For comparison purpose to show the effect of sweep voltages on the statistical time-lag distribution of the impulse breakdown voltage data, it is more illustrative to indicate all time-lag data in the form of 'Laue' plots [25].

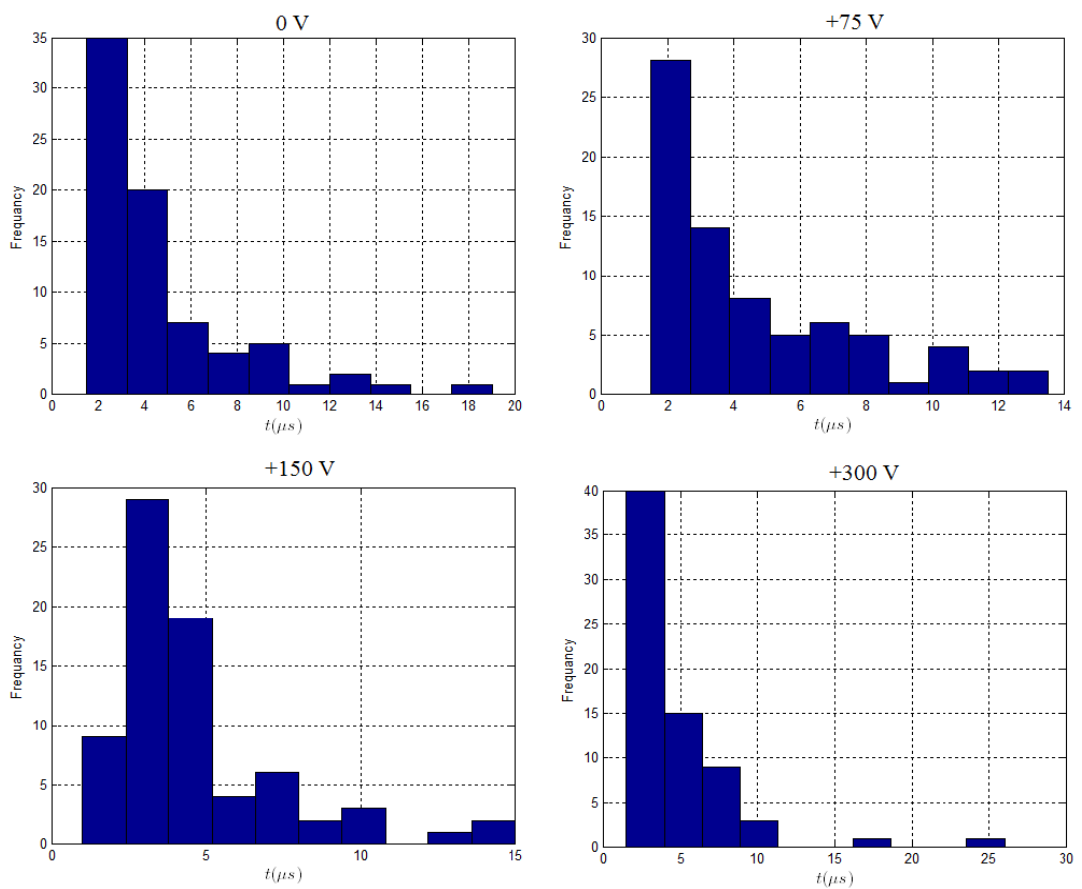


Figure 4. 19 Histograms of statistical time-lag data for various positive sweep voltages.

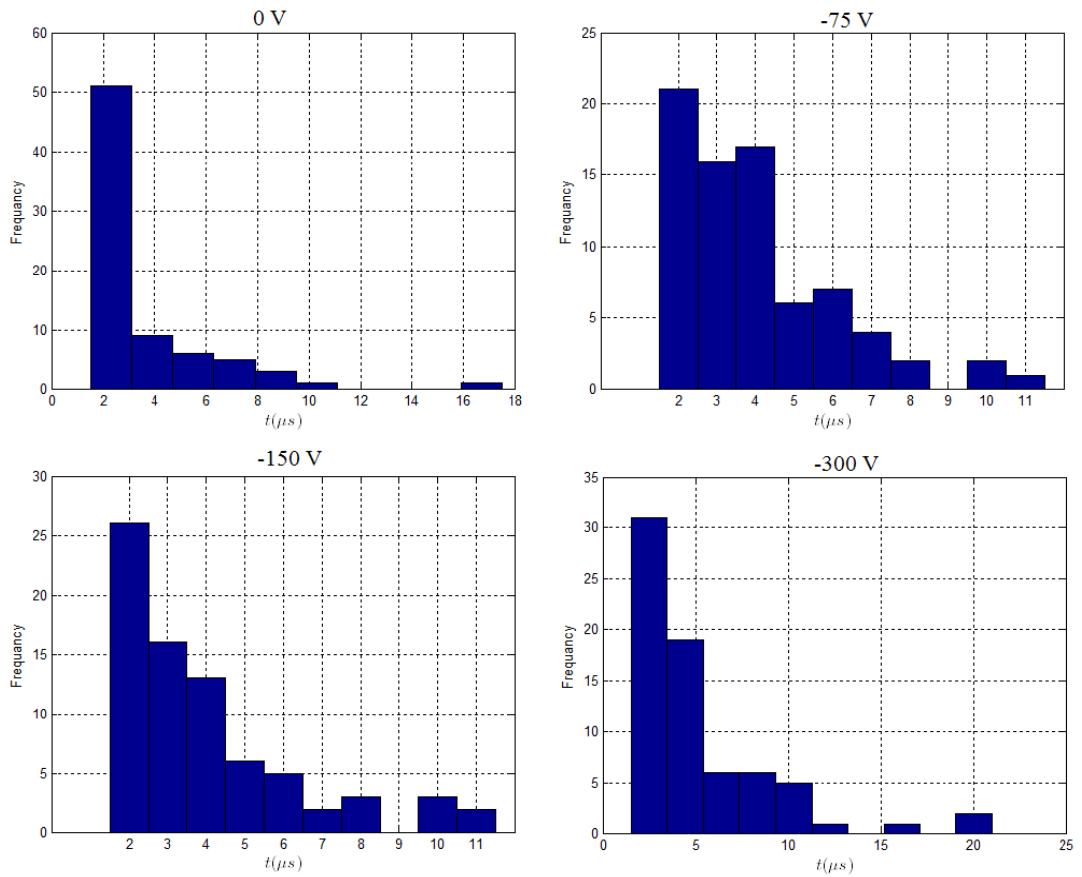


Figure 4. 20 Histograms of statistical time-lag data for various negative sweep voltages.

The distributions of time-lag data are illustrated in the form of ‘Laue’ plots in Figures 4.21 and 4.22. As was mentioned in Section 2.2, the slopes of these plots should be proportional to the rate of production of free electrons which is correlated to the negative ion density in the region of the tip of the rod [10], hence, appearance of negative ions within the critical volume prior to application of the impulse voltage.

The distributions of statistical time-lag data with and without a positive and negative sweep voltage are very close to each other. This phenomena clearly displayed in ‘Laue’ plots shown in Figure 4.21 under the effect of positive sweep voltages and in Figure 4.22 for negative sweep voltages. In both figures, statistical time-lags do not show any tendency to change with increasing sweep voltage. The reason for this is probably due to the fact that the tip of the rod-plane test gap is always left to the

natural radiation, contrary to the works in the literature performed under continuous external radiative illumination [10, 11].

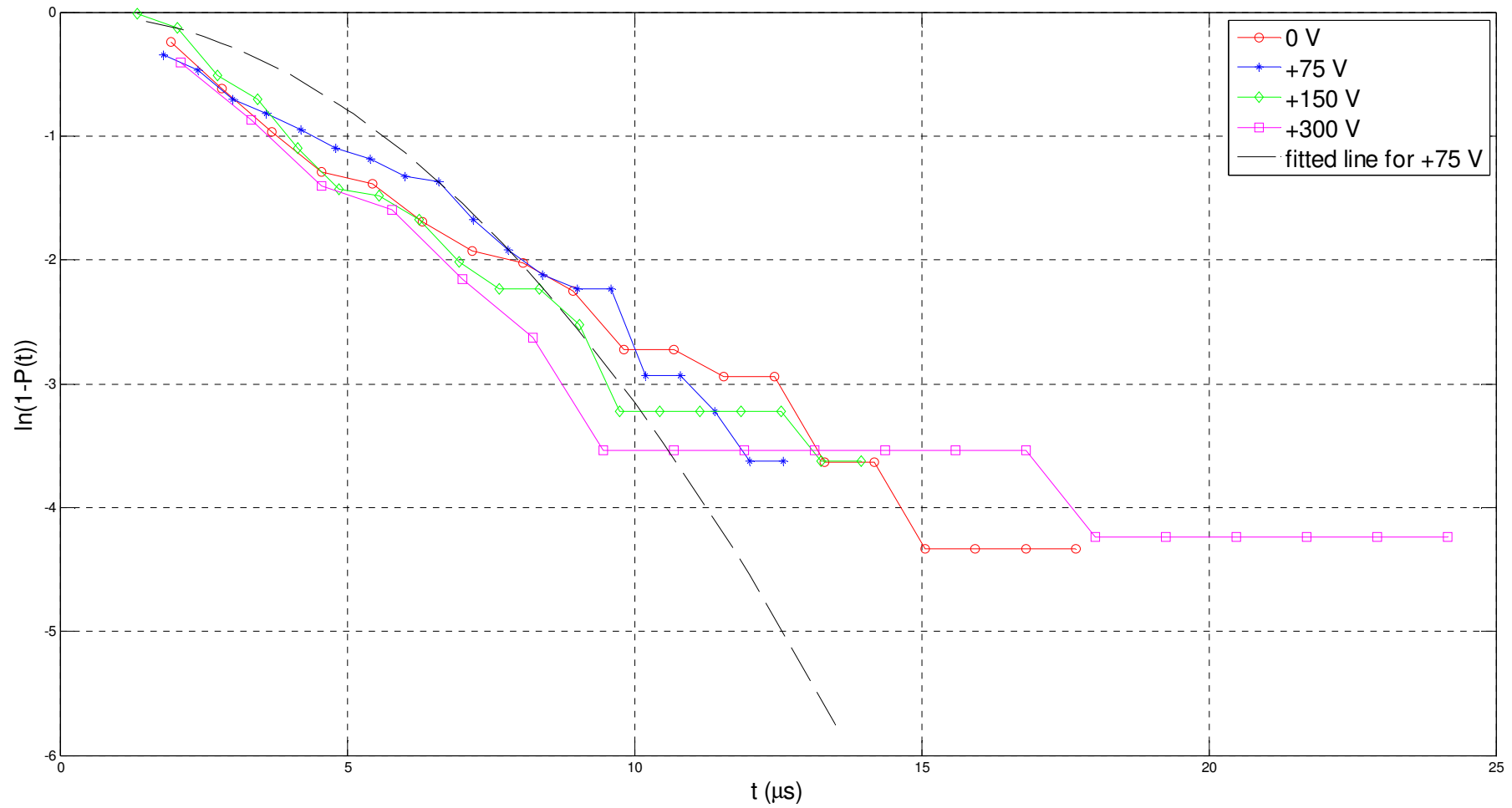


Figure 4.21 Laue plots for the rod-plane test gap for various positive sweep voltages.

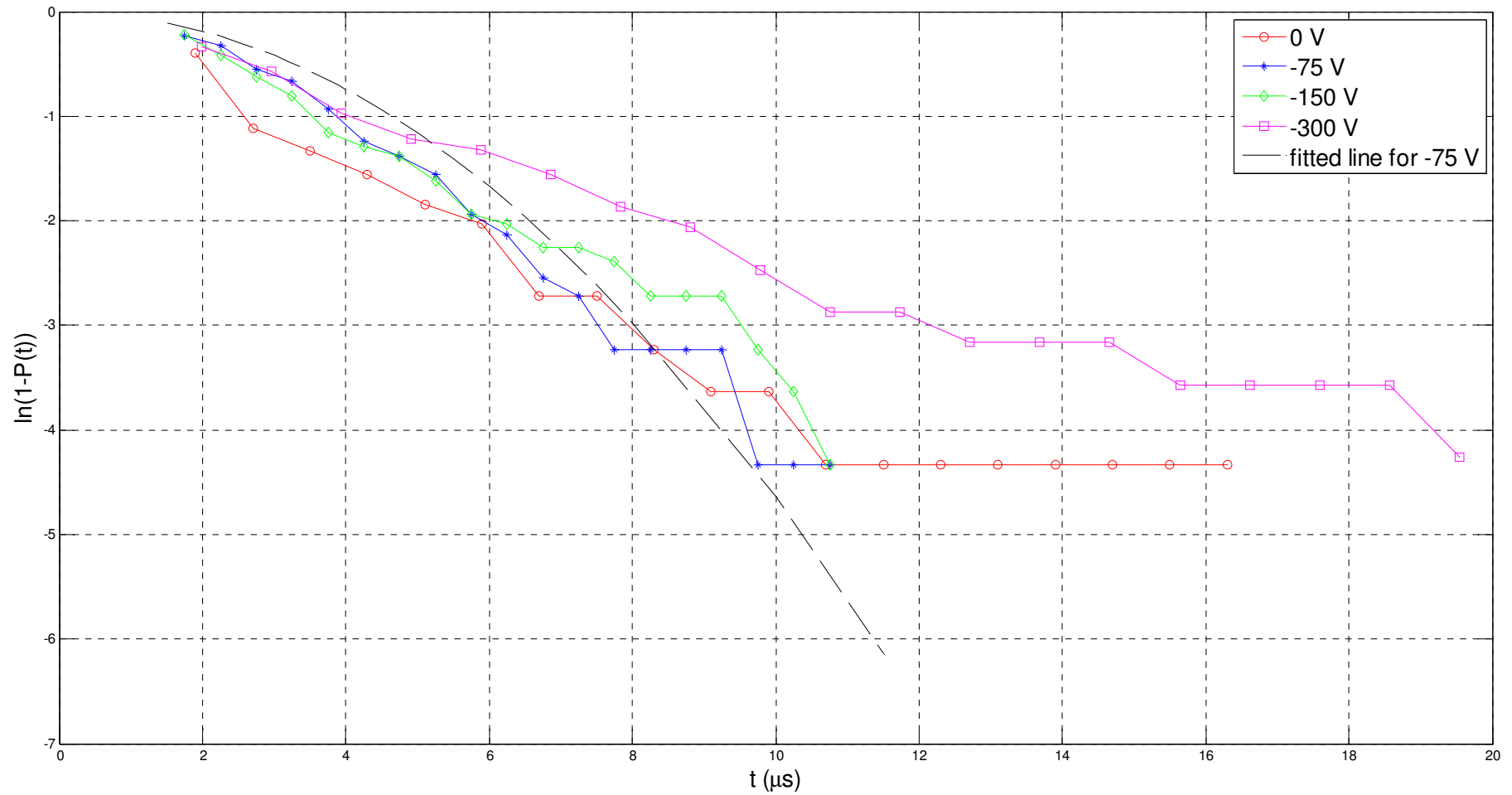


Figure 4.22 Laue plots for the rod-plane test gap for various negative sweep voltage.

As shown in Figures 4.21 and 4.22, the slopes of Laue plots of statistical time-lag distributions for +75 V and -300 V sweep voltages are less steeper than the other distributions of the same polarity set. Correspondingly, 50% impulse breakdown voltages for +75 V and -300 V are also greater than others. We can conclude that there is a clear correlation between statistical time-lag distributions and the values of 50% impulse breakdown voltage.

.

CHAPTER V

CONCLUSION

The impulse breakdown voltage data obtained from up-and-down tests in the literature is generally thought to follow normal or 3PW probability distributions in different test gap systems. However, in the present study, the distribution of impulse breakdown voltage data obtained in air-insulated rod-plane systems under the various DC sweep voltages is generally found to follow the logistic distribution. Comparison of the the logistic distribution with the normal, 3PW and Gumbel distributions under the effect of DC sweep voltages indicated that Gumbel distribution is inappropriate for all present up-and-down test data, and logistic distribution can sometimes perform better than normal and 3PW probability distributions.

The normal and 3PW probability distributions although are generally accepted to represent the statistical characteristics of self-restoring insulation systems, as a result of this study it is proved that logistic distribution may be suggested to be as an alternative to these distributions.

Under the same test conditions both the statistical time-lag distributions and the corresponding 50% impulse breakdown voltages are found to be not affected with the DC sweep voltage. It is also denoted that there is a strong correlation between statistical time-lag distribution and the value 50% impulse breakdown voltage.

During tests, the unexpected deviations in the distributions of the impulse breakdown data under positive sweep voltage +75 V is probably due to the close weather conditions during the experiments; the shielding effect of the clouds for the cosmic ray flows [25] is known to be restrictive. Hence, excluding the variations caused by

the +75 V sweep voltage, the logistic distribution can be a definitive alternative to the generally accepted normal and 3PW probability distributions.

REFERENCES

- [1] Lucas, J.R. (2001). High Voltage Engineering. Available via URL. http://elect.mrt.ac.lk/pdf_notes.htm.
- [2] IEEE Std 4-1995 (1995). IEEE Standard Techniques for High-Voltage Testing. The Institute of Electrical and Electronics Engineers. New York
- [3] Glover, J.D., Sarma, M. (1994). Power System Analysis and Design. 2nd Edition. Boston: PWS Publishing Company, pp. 510-515.
- [4] Bakken, J.A. (1967). Determination of characteristic voltages in impulse and switching surge testing. *IEEE Transactions on Power Apparatus and Systems*. 86(8), pp. 962–968.
- [5] Wibholm, S., Thyregod P. (1986). The analysis of insulation breakdown probabilities by the up-and-down method. *IEEE Transactions on Electrical Insulation*. 21, pp. 133–136.
- [6] IEC Pub. 60060-2. (1989). High-Voltage Test Techniques. Part 2: Test Procedures. International Electrotechnical Commission.
- [7] Dixon, W.J., Mood, A.M. (1948). A method for obtaining and analyzing sensitivity data. *Journal of American Statistical Association*. 43, pp. 109-126.
- [8] Kouno, T., Oikawa, T. (1967). Standard Deviation of Flashover Probability. *Journal of International Electrical Engineers*. 87, pp. 84-89.

- [9] Meek, J.M., Craggs, J.D. (1978). *Electrical Breakdown of Gases*. New York: John Wiley & Sons, pp. 655-661.
- [10] Somerville, I.C., Tedford, D.J. (1979). The spatial and temporal variation of ion densities in non-uniform-field gaps subjected to steady state or transient voltages. 3rd Int. Symp. On High Voltage Engineering. IEE Publ., 2, pp. 53.02.
- [11] Somerville, I.C., Tedford, D.J. (1978). Time-lags to breakdown: The detachment of atmospheric negative ions. 5th Int. Conf. On Gas Discharges. IEE Publ., 165, pp. 250-253.
- [12] Hirose, H. (2007). More accurate breakdown voltage estimation for the new step-up test method in the Gumbel distribution model. *European Journal of Operational Research*. 177, pp. 406-419.
- [13] Hirose, H. (2003). More accurate breakdown voltage estimation for the new step-up test method. *IEEE Transactions on Dielectrics and Electrical Insulation*. 10(3), pp. 475-482.
- [14] Hirose, H. (2004). More accurate breakdown voltage estimation for the new step-up test method in the Weibull model. *IEEE Transactions on Dielectrics and Electrical Insulation*. 11(3), pp. 418-423.
- [15] Yildirim, F., Korasli, C. (1992). Statistical approach for determining breakdown voltage of gas-insulated cables. *IEEE Transactions on Electrical Insulation*. 27, pp. 1186-1192.
- [16] Korasli, C. (1998). Statistical inference for breakdown voltage in SF₆ GIS from first breakdown data. *IEEE Transactions on Dielectrics and Electrical Insulation*. 5(4), pp. 596-602.
- [17] Zhang, Y., Liu, Z., Geng, Y., Yang, L., Wang, J. (2011). Lightning impulse voltage breakdown characteristics of vacuum interrupters with contact gaps 10 to 50 mm. *IEEE Transactions on Dielectrics and Electrical Insulation*. 18, pp. 2123-2130.

- [18] Vibholm, S., Thyregod, P. (1988). A study of the up-and-down method for non-normal distribution functions. *IEEE Transactions on Electrical Insulation*. 23, pp. 357-364.
- [19] Marques de Sá, J.P. (2007). Applied Statistics using SPSS, Statistica, MATLAB and R. 2nd Edition. Berlin Heidelberg: Springer-Verlag. pp. 183-186.
- [20] Abouammoh, A.M., Alshingiti, A.M. (2009). Reliability estimation of generalized inverted exponential distribution. *Journal of Statistical Computation and Simulation*. 79, pp. 1301–1315.
- [21] Lu, W., Shi, D. (2012). A new compounding life distribution: The Weibull–Poisson distribution. *Journal of Applied Statistics*. 39, pp. 21-38.
- [22] Gupta, R.D., Kundu, D. (2001). Exponentiated exponential family: An alternative to gamma and Weibull distributions. *Biometrical Journal*. 43, pp. 117–130.
- [23] Chapra, S.C. (2006). Numerical Methods for Engineers. 6th Edition. Mc Graw Hill. pp. 355-374.
- [24] Kuffel, E., Zaengl, W.S., Kuffel, J. (2000). High Voltage Engineering Fundamentals. 2nd Edition. Oxford: Newnes. pp. 52-60.
- [25] Laue, M., V. (1925). *Annual Physics*. 76, pp. 261.
- [26] Gaiser, T., K. (1990). Cosmic Rays and Particle Physics. First Edition. Cambridge University Press.

APPENDICES

A.1 Numerical Solution of Log-Likelihood Equations

The LL equations need to be solved numerically. The numerical solution of LL equation systems is very hard to solve owing to the nonlinear nature of the equations and numerical solutions are strongly dependent upon the initial values of parameter estimates. Newton-Raphson method is used to determine the parameter estimates of LL equations

In Newton-Raphson method, Hessian matrix and gradient should be formed. Mostly, probability distribution functions have parameters more than one. For this reason, LL function is multi-dimensional.

$p(v;\theta)$ is the probability density function. (v_1, \dots, v_n) is the random sample on a random variable v and $(\theta_1, \dots, \theta_m)$ are the population parameters. v voltage values are taken from up-and-down tests in the laboratory. θ is the parameters of distribution function like μ and σ in normal distribution function. m is the number of parameters in probability density function.

Gradient is the first derivative of LL function in maximum likelihood method. Gradient tells us that it is the slope of the LL function and also represents the directional derivative of LL function at the specific point. The first derivative of LL equation is taken with respect to each parameter to form gradient vector. The first derivative of log-likelihood function provides a steepest trajectory of the function and tells us that we have reached an optimum point. In the matrix format, it is shown in Equation (A.1) [23];

$$\nabla(\ln(L)) = \begin{bmatrix} \frac{\partial(\ln(L))}{\partial\theta_1} \\ \frac{\partial(\ln(L))}{\partial\theta_2} \\ \cdot \\ \cdot \\ \frac{\partial(\ln(L))}{\partial\theta_m} \end{bmatrix} \quad (\text{A.1})$$

Hessian matrix is formed by taking the second derivative of LL function with respect to parameters. The second derivative tells us whether we are at a maximum or a minimum if optimum point is reached by the first derivatives. If the partial second derivatives with respect to all parameters are negative, then the maximum is reached. But this is not always true. The reached point may also be a saddle point. At the saddle point derivative is zero but it is not a maximum nor a minimum [23]. Hessian matrix (\mathbf{H}) format is given by;

$$\mathbf{H} = \begin{bmatrix} \frac{\partial^2 \ln(L)}{\partial\theta_1^2} & \frac{\partial^2 \ln(L)}{\partial\theta_1\partial\theta_2} & \cdot & \cdot & \cdot & \frac{\partial^2 \ln(L)}{\partial\theta_1\partial\theta_m} \\ \frac{\partial^2 \ln(L)}{\partial\theta_2\partial\theta_1} & \frac{\partial^2 \ln(L)}{\partial\theta_2^2} & \cdot & \cdot & \cdot & \frac{\partial^2 \ln(L)}{\partial\theta_2\partial\theta_m} \\ \cdot & & \cdot & & & \\ \cdot & & & \cdot & & \\ \cdot & & & & \cdot & \\ \frac{\partial^2 \ln(L)}{\partial\theta_m\partial\theta_1} & \frac{\partial^2 \ln(L)}{\partial\theta_m\partial\theta_2} & \cdot & \cdot & \cdot & \frac{\partial^2 \ln(L)}{\partial\theta_m^2} \end{bmatrix} \quad (\text{A.2})$$

After Hessian and gradient matrices are formed, the points that provide maximum value of LL are found. The vector which include parameters of probability density function is given by;

$$\boldsymbol{\theta} = \begin{bmatrix} \theta_1 \\ \theta_2 \\ \cdot \\ \cdot \\ \cdot \\ \theta_m \end{bmatrix} \quad (\text{A.3})$$

To find the optimum parameter values, Equation. (2.24) is produced.

$$\boldsymbol{\theta}_{i+1} = \boldsymbol{\theta}_i - \mathbf{H}_i^{-1}(\nabla \ln(L))_i \quad (\text{A.4})$$

If proper initial values are entered, this algorithm finds optimum values easily. This method can also find local minimum or local maximum points on the LL function. For this reason, this method cannot always find correct results.

A.1.1 Main Algorithm for Newton-Raphson Method

At the beginning of the program, initial parameter values and tolerance are wanted from the user, and the iteration number k is equated to zero. In this program, ‘while loop’ is formed and there are two conditions of this loop to terminate. One is the difference between previous and current parameter values, and the other is maximum allowed iteration number N . k is incremented at each iteration. If iteration number reaches 1000, then loop is terminated automatically. After k is incremented, Hessian and gradient matrices are computed in different two functions. The results of these matrices are inserted to Equation (A.4) and parameter values are calculated. Later on, current parameter values are subtracted from the preceding parameter values. Provided that difference is small than tolerance, then condition is satisfied and loop is terminated. Otherwise, loop continues until finding optimum parameter values. As soon as loop is finished, results are displayed on command window of MATLAB. Flow chart of this algorithm is shown in Figure A.1.

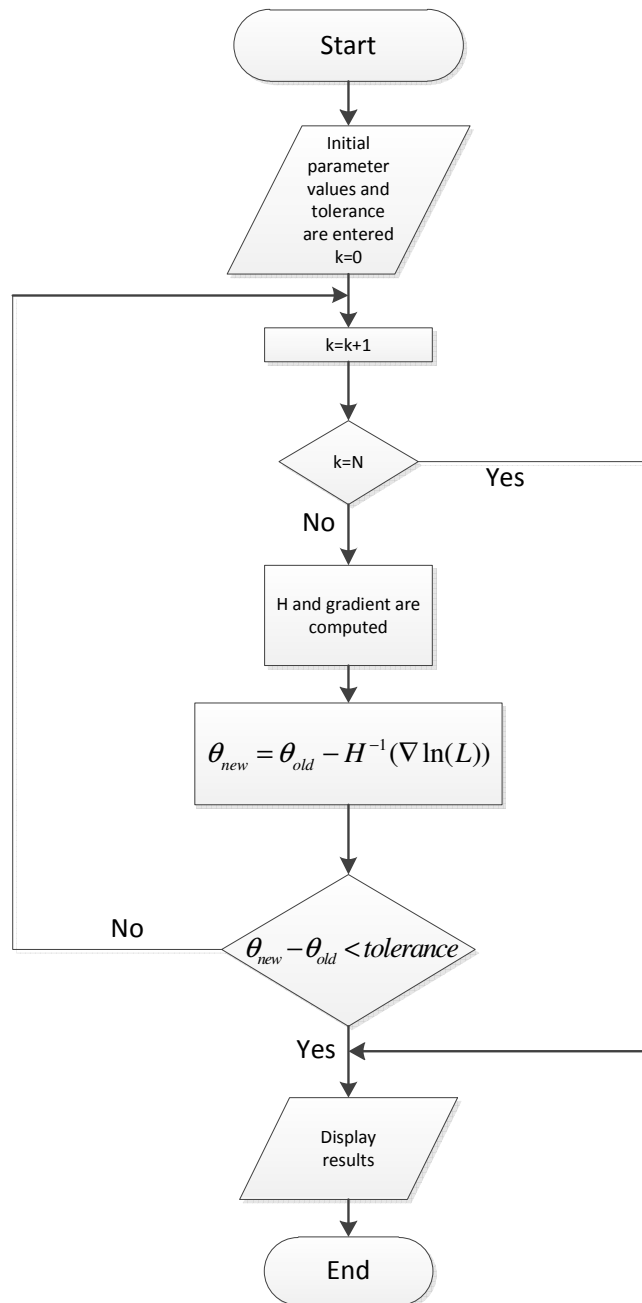


Figure A.1 Flow chart of Newton-Raphson Method.

A.2 Monte Carlo Optimization of Log-likelihood Equations

MC optimization method repeatedly computes the function at randomly selected values of the independent variables. Random numbers are generated in particular intervals for each parameter using **rand** command in MATLAB. After random numbers generated, these values are substituted into the LL function. It searches for maximum value of the function. If a sufficient number of samples are conducted, the optimum values can be found [23].

This method works properly for discontinuous and nondifferentiable functions. This method always finds global maximum rather than a local maximum. The major disadvantage of this method is that as the number of independent variables raises, the implementation effort required can become cumbersome [23]. The other disadvantage of this method is slower than other numerical methods. To find the parameter estimates exactly, the iteration number should be increased.

A.2.1 Main Algorithm for Monte Carlo Optimization Method

In this algorithm, firstly variable $\max \ln(L)$ and parameter values are initiated. $\max \ln(L)$ should have a very small negative value. ‘while loop’ is used in this program. k is incremented at each iteration. There is only one condition to terminate the loop. If k reaches N , loop is terminated. N is important variable in this algorithm. The bigger the value of N , the more accurate parameter values are obtained. Random values are produced in determined interval for parameters and assigned to parameter variables of selected probability distribution function at each iteration. Provided that new value of log-likelihood function is greater than the previous one, the new values for parameters are captured. At the end of iteration, the parameter values that make maximum the LL function is displayed. Flow chart of this algorithm is shown in Figure A.2.

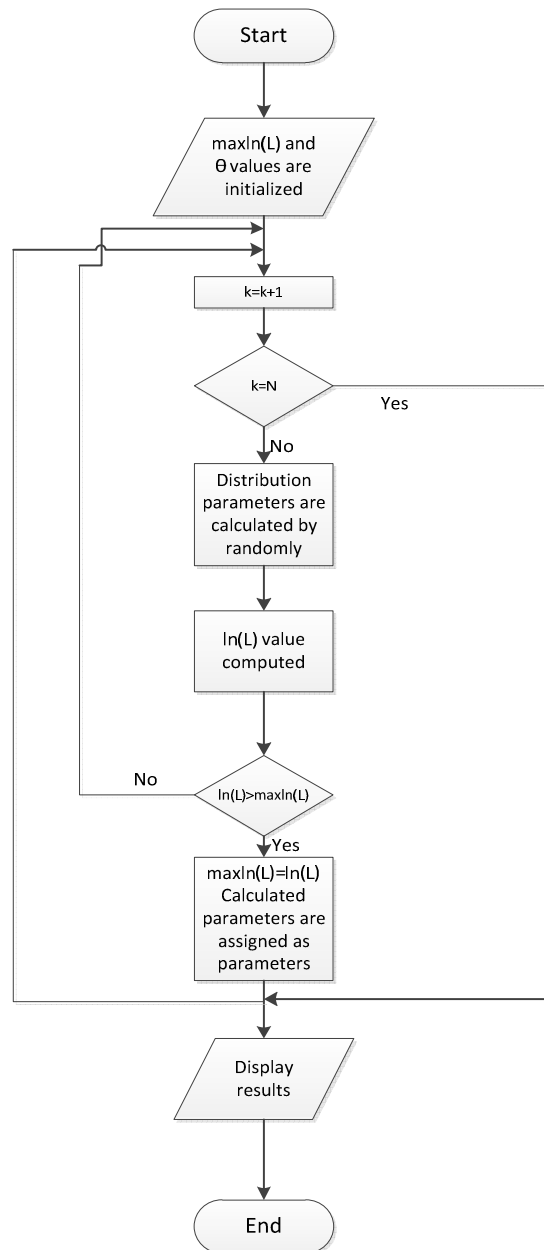


Figure A.2 Flow chart of Monte Carlo Optimization.

A.3 Generation of Impulse Voltages

A.3.1 Impulse Voltage Generator Circuits

The fast increase and slow decay in impulse voltages can be accomplished by impulse voltage generator circuits. Capacitors should be used for charging and discharging in these circuits. The waveshape of impulse voltages may mathematically be described as superposition of two exponential functions [24].

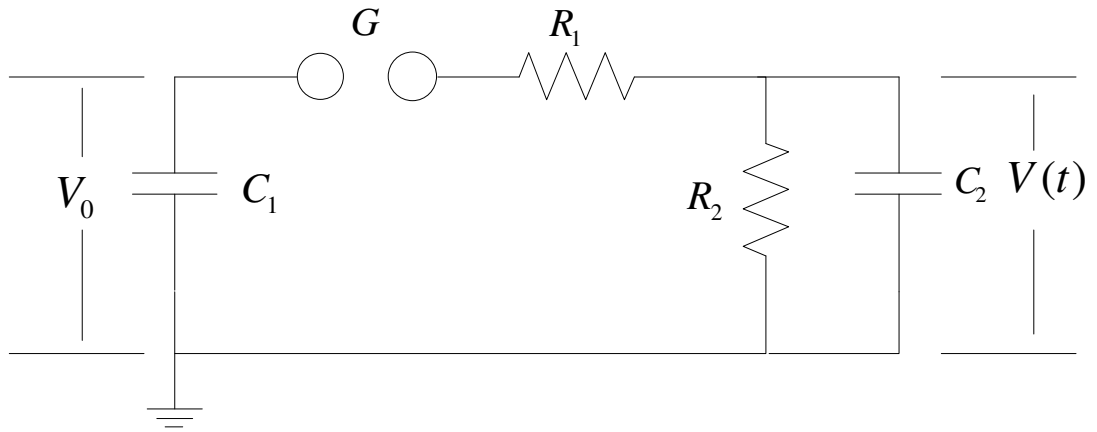
The introduction to the full impulse voltages as defined in chapter 1 leads to simple circuits for the generation of the necessary waveshapes. The rapid increase and slow decay can obviously be generated by discharging circuits with two energy storages, as the waveshape may well be composed by the superposition of two exponential functions [24]. The mathematical expression of standard lightning impulse can be given by following Equation (3.1)

$$V(t) = V_0[\exp(-\alpha_1 t) - \exp(-\alpha_2 t)] \quad (\text{A.5})$$

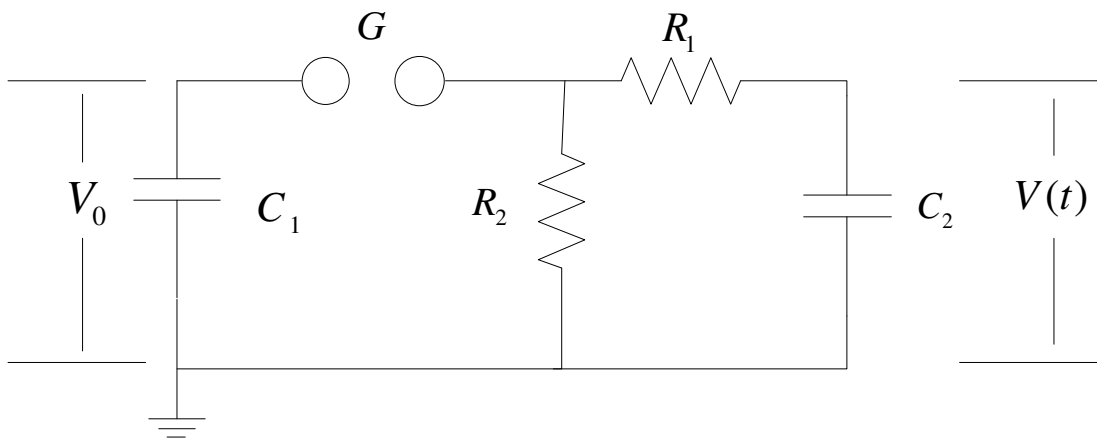
For the standard 1.2 / 50 μs lightning impulse waveshape, α_1 should be $1.46 \cdot 10^4 \text{ s}^{-1}$ and α_2 should be $2.47 \cdot 10^6 \text{ s}^{-1}$ [2]. The load of impulse generators are capacitive, while insulation systems are being tested. This load will contribute to the stored energy. A suitable fast discharge circuit always consist essentially two capacitors [24].

A.3.1.1 Single-Stage Impulse Generator Circuits

As shown in Figure A.3, there are two basic circuits for single-stage impulse generators. C_1 is slowly charged by a d.c. source until spark G breakdowns. After ignition time of spark gap G, first capacitor C_1 starts discharging. To obtain d.c. voltage at the input of the circuit, half-wave or full-wave rectifier circuits are used. The ignition time of spark gap is very low according to rising time T_1 . Resistors R_1 and R_2 and capacitor C_2 are used to form the waveshape of LI voltages. R_1 determines the rising time T_1 , so that R_1 primarily damps the circuit. R_2 will discharge the capacitors and control the wavetail of the impulse waveshape. C_2 is assumed full load of the circuit, the capacitance of test object and other capacitive elements are ignored. Inductances are also ignored to understand the principals of these impulse generator circuits [24].



(a)



(b)

Figure A.3 Single-stage impulse generator circuits.

We may use the Laplace transform technique to analyze the circuit. For $t \leq 0$, C_1 is charged to V_0 and for $t > 0$ this capacitor is directly connected to the wave shaping circuit. The output voltage is given by [24];

$$V(s) = \frac{V_0}{s} \frac{Z_2}{Z_1 + Z_2} \quad (\text{A.6})$$

where

$$Z_1 = \frac{1}{C_1 s} + R_1 \quad (\text{A.7})$$

$$Z_2 = \frac{R_2 / C_2 s}{R_2 + 1 / C_2 s} \quad (\text{A.8})$$

By substitution we find

$$V(s) = \frac{V_0}{k} \frac{1}{s^2 + as + b} \quad (\text{A.9})$$

where

$$a = \left(\frac{1}{R_1 C_1} + \frac{1}{R_1 C_2} + \frac{1}{R_2 C_2} \right) \quad (\text{A.10})$$

$$b = \left(\frac{1}{R_1 R_2 C_1 C_2} \right) \quad (\text{A.11})$$

$$k = R_1 C_2 \quad (\text{A.12})$$

For circuit Figure A.3 (b) the same general expression can be obtained by small differences.

$$a = \left(\frac{1}{R_1 C_1} + \frac{1}{R_1 C_2} + \frac{1}{R_2 C_1} \right) \quad (\text{A.13})$$

$$b = \left(\frac{1}{R_1 R_2 C_1 C_2} \right) \quad (\text{A.14})$$

$$k = R_1 C_2 \quad (\text{A.15})$$

For both circuits, we obtain the same expression in time domain.

$$V(t) = \frac{V_0}{k} \frac{1}{\alpha_2 - \alpha_1} [\exp(-\alpha_1 t) - \exp(-\alpha_2 t)] \quad (\text{A.16})$$

$$\alpha_1, \alpha_2 = \frac{a}{2} \mp \sqrt{\left(\frac{a}{2}\right)^2 - b} \quad (\text{A.17})$$

The output voltage $V(t)$ is the superposition of two exponential functions of different signs [24].

A.4 Normalization of Up-and-down Test Data to STP Conditions

The normalization of the up-and-down test data to STP conditions is done by Equation A.18

$$V_{act} \cdot \frac{k_h}{k_d} = V_{STP} \quad (\text{A.18})$$

where k_h is a graphical constant obtained from BS 923:1972 and $k_d = \frac{p}{p_o} \cdot \frac{273+t_o}{273+t}$.

(p : Ambient pressure, t : Ambient temperature, p_o : Pressure at STP, t_o : Temperature at STP).